ıIC STRATIGRAPHY OF LATE QUATERNARY SEDIMENTS ON THE CONTINENTAL SHELF OF ANTALYA BAY

A Thesis submitted to

INSTITUTE OF MARINE SCIENCES
MIDDLE EAST TECHNICAL UNIVERSITY

by
DEVRİM TEZCAN

In partial fulfillment of the requirements for the degree of

MASTER OF SCIENCE
in
MARINE GEOLOGY AND GEOPHYSICS

September 2001
İÇEL / TÜRKİYE

Approval of the Graduate School of MARINE SCIENCES

Prof. Dr. İlkay SALİHOĞLU
Director

I certify that this thesis satisfies all the requirements as a thesis for the degree of Master of Science.

Assoc. Prof. Dr. Mahmut OKYAR
Head of Department of Marine Geology and Geophysics

This is to certify that we have read this thesis and that in our opinion it is fully adequate, in scope and quality, as a thesis for the degree of Master of Science.

Assoc. Prof. Dr. Mahmut OKYAR
Supervisor

Other Members of Examining Committee

Prof. Dr. Süleyman TUĞRUL

Prof. Dr. Temel OĞUZ

Prof. Dr. Ayşen YILMAZ

Assist. Prof. Dr. Vedat EDİGER

ABSTRACT

SEISMIC STRATIGRAPHY OF LATE QUATERNARY SEDIMENTS ON THE CONTINENTAL SHELF OF ANTALYA BAY

TEZCAN, Devrim
M.Sc., Department of Marine Geology and Geophysics
Supervisor: Assoc.Prof.Dr. Mahmut OKYAR
September 2001, 62 pages

The present bathymetry and Late Quaternary stratigraphy of the continental shelf of the Antalya Bay has been investigated by using echo-sounding and high-resolution shallow seismic profiling methods.

In general, the isobath lines, representing the sea floor topography, lie conformably with the coastline of the Antalya Bay. Gently sloping (< 2°) wide shelf areas are the important characteristics of the western and northern regions of the Antalya Bay. This peculiarity indicates high sediment supply to these shelf areas from the rivers on the land. In contrast to this, the eastern region of the Antalya Bay is marked by steeply sloping (>2°) shelf. This configuration of bathymetry is basically controlled by sedimentation and tectonics of the Antalya Bay. Submarine canyons and topographic irregularities appear to be other prominent features of the sea floor in the Antalya Bay.

Based on the seismic stratigraphic approach, four distinct depositional sequences (1, 2, 3, and 4) above the acoustic basement (AB) have been identified in the sub sea-floor of the Antalya Bay. Additionally, a basal reflector-R that forms the boundary between the pre-Holocene and the Holocene sequences was interpreted.

The acoustic basement, exhibiting chaotic reflection configurations, consists of the seaward extension of onshore sequences. Therefore, its composition varies from place to place. In some regions, acoustic basement has been faulted.

The depositional sequence 1 is characterized by chaotic and parallel-subparallel reflection configurations. It overlies the acoustic basement and pinches out landward at the depth of 75 m below the present sea level. Available sea level curve for the eastern Mediterranean Sea reveals that this level correspond to 22 000 yrs B.P. Therefore, depositional sequence 1 is interpreted to be pre-Holocene in age.

The depositional sequence 2, showing chaotic and oblique progradational reflection patterns, pinches out at the depth of 110 m on the reflector-R. This sequence has been deposited during the earlier stage of Holocene transgression between 22 000 and 18 000 yrs B.P., on the basis of the sea level curve. This sequence is not observed in some areas where uplift and erosion processes are common. The maximum thickness of sequence 2 is measured to be as 40 meters.

The depositional sequence 3, underlying depositional sequence 4, represents chaotic and parallel-subparallel reflection configurations. It pinches out at the depth of 50 m on reflector-

R, which corresponds to approximately 11 500 yrs B.P. on available sea level curve. This sequence has been formed during the period from about 18 000 yrs B.P. until 11500 yrs B.P. Depositional sequence is not observed in some areas due to similar processes, explained above paragraph. The maximum thickness of sequence 3 is reached to 50 meters.

Depositional sequence 4, resembling seaward sedimentary wedge, is the youngest seismostratigraphic unit of the surveyed area. Its upper boundary forms the present sea floor. This sequence has been accumulating for the last 11 500 yrs B.P. Its thickness tends to increase ($\geq$ 40 m) in front of the fan-delta areas.

The basal reflector-R, forming the boundary between the pre-Holocene sequence (1) and the Holocene sequences (2, 3 and 4), is interpreted as pre-Holocene erosional surface produced by the subaerial fluvial erosion of the continental shelves.

ÖZET

ANTALYA KÖRFEZİ KITA SAHANLIĞININ GEÇ KUVATERNER SEDİMANLARININ SİSMİK STRATİGRAFİSİ

TEZCAN, Devrim
Yüksek Lisans Tezi, Deniz Jeolojisi ve Jeofiziği Anabilimdalı
Tez Danışmanı: Doç.Dr. Mahmut OKYAR
Eylül 2001, 62 sayfa

Antalya Körfezi'nin kıta sahanlığının güncel batimetrisi ve geç Kuvaterner stratigrafisi, ses yankılaması ve yüksek ayırımlı sığ sismik yöntemler kullanılarak araştırılmıştır.

Genel olarak, deniz tabanının topografyasını temsil eden eşderinlik eğrileri Antalya Körfezinin kıyı şeridine uyumlu bir şekilde uzanmaktadır. Hafif eğime sahip (<2°) geniş kıta sahanlıkları Antalya Körfezi'nin kuzey ve batı bölgelerinin önemli karakteristik özelliğidir. Bu özellik nehirler aracılığıyla, karadan denize yüksek miktarda sediman taşınımı olduğunu göstermektedir. Buna karşılık, Antalya Körfezi'nin doğu bölgesi oldukça dik eğime sahip (>2°) kıta sahanlığı ile temsil edilmektedir. Batimetrinin bu şekli temel olarak sedimantasyon ve Antalya Körfezi'nin tektoniği ile kontrol edilmektedir. Deniz altı kanyonları ve topografik düzensizlikler Antalya Körfezi deniz tabanının diğer göze çarpan özellikleridir.

Sismik stratigrafik yaklaşımla, Antalya Körfezinde, deniz tabanının altında, akustik temelin (AB) üstünde yer alan dört farklı çökel serisi (1,2,3 ve 4) tespit edilmiştir. Buna ilave olarak, Holosen ve Holosen öncesi serileri ayıran bir R taban reflektörü belirlenmiştir.

Karışık yansıma şekilleri ile tanımlanan akustik temel, karadaki birimlerin denize doğru uzanımlarıdır. Bu yüzden, bileşimi bölgeden bölgeye farklılık göstermektedir. Bazı yerlerde, akustik temel faylarla kesilmiştir.

Çökel serisi 1 karmaşık ve paralel-az paralel yansıma şekilleri ile tanımlanmıştır. Akustik temelin üzerinde yer alıp, bugünkü deniz seviyesinden 75 m aşağıda kara tarafına doğru sona ermektedir. Doğu Akdeniz için mevcut olan deniz seviyesi değişim eğrisi, bu derinliğin günümüzden yaklaşık 22 000 yıl öncesine karşılık geldiğini ortaya koymaktadır. Bu yüzden çökel birimi 1, Holosen öncesi yaşlı bir birim olarak yorumlanmıştır.

Karmaşık ve oblik yansıma şekilleri ile tanımlanan çökel serisi 2, R reflektörünün üzerinde 110 m derinlikte sona ermektedir. Deniz seviyesi değişim eğrisine göre, bu seri Holosen trangresyonunun başlarında, günümüzden 22 000 öncesinden 18 000 yıl önceki zaman aralığında çökelmiştir. Erozyonun ve yükselmenin olduğu bölgelerde bu seri gözlenmemiştir. Çökel serisi 2'nin en fazla kalınlığı 40 metredir.

Çökel serisi 4'ün altında uzanan, çökel serisi 3, karmaşık ve paralel-az paralel yansıma şekilleri ile tanımlanmıştır. Bugünkü deniz seviyesinden yaklaşık 50 m derinlikte R reflektörü üzerinde sona eren bu seri, günümüzden yaklaşık 18 000 yıl öncesinden 11 500 yıl öncesine

kadar olan zamanda çökelmiştir. Yukarıdaki paragrafta bahsedilen nedenlerden dolayı, çökel serisi 3'de bazı yerlerde gözlenememiştir. Çökel serisi 3 ün azami kalınlığı 50 m ye ulaşmaktadır.

Denize doğru bir sediman kamalanmasını temsil eden çökel serisi 4, çalışma sahasındaki en genç sismostratigrafik birimdir. Bu serinin üst sınırı günümüz deniz tabanını oluşturmaktadır. Son 11 500 yılda çökelen bu serinin kalınlığı, fan-delta bölgelerinde artma eğilimi (≥40 m) göstermektedir.

Holosen dönemi çökel serileriyle (2,3 ve 4), Holosen öncesi dönem çökel serisini (1) ayıran R- taban reflektörü, kıta sahanlığının havaaltı akarsu erozyonuna maruz kalmasıyla oluşan, Holosen öncesi aşınım yüzeyi olarak yorumlanmıştır.

ACKNOWLEDGMENTS

I express sincere appreciation to Assoc. Prof. Dr. Mahmut OKYAR for his guidance, helps and suggestions during my thesis.

I would like to thank to Prof. Dr. İlkay SALİHOĞLU for providing ship time and research facilities.

I am grateful to Assist. Prof. Dr. Vedat EDİGER for his valuable comments and suggestions.

I would also like to thank to Electronical Engineer Mehmet DEMİREL for his help during data collection.

I wish to express my appreciation to the crew of the R/V Bilim for their help in collecting data.

I would also like to thank my family for their continuous encouragements and helps.

CONTENTS **page**

LIST OF TABLES

LIST OF FIGURES

CHAPTER ONE
INTRODUCTION

1.1 General characteristics of the study area

The study area is located in Antalya Bay (Figure 1.1). It extends seaward from between Cape Taşlık and Gazipaşa (Figure 1.1).

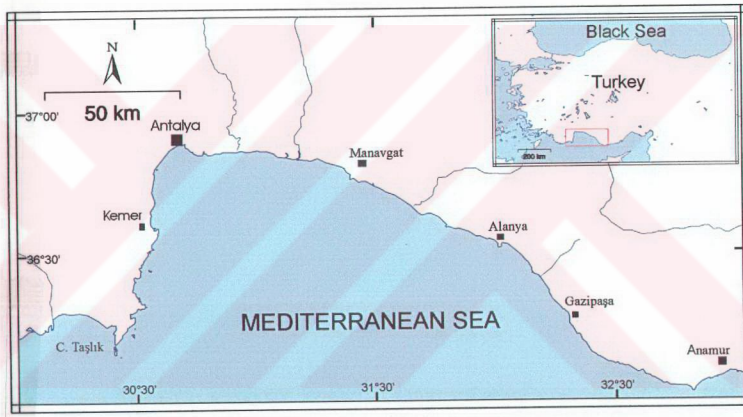

Figure 1.1: Location map of the study area.

1.2 Physiography and coastal morphology of the Antalya Bay

Antalya Bay and the surrounding region are characterized by high mountains, which plunge precipitously into the Mediterranean Sea to form a coastline dominated by sea cliffs (Evans, 1970).

The Taurids, tectonic belt of the Southern Turkey, is an important link in the Alpine – Himalayan mountain range (Bremer, 1971). The western part of the Taurids that extends

from Aegean coast to Anamur, is divided into two branches (Figure 1.2) formed a marked angle enclosing the Antalya Bay (Brunn *et al.*, 1971). The eastern branch is oriented in NW- SE direction and is named as Taurus Occidental (Blumenthal, 1947). The other branch is oriented in NE – SW direction and is named as Lycian Taurus (Brunn *et al.*, 1971).

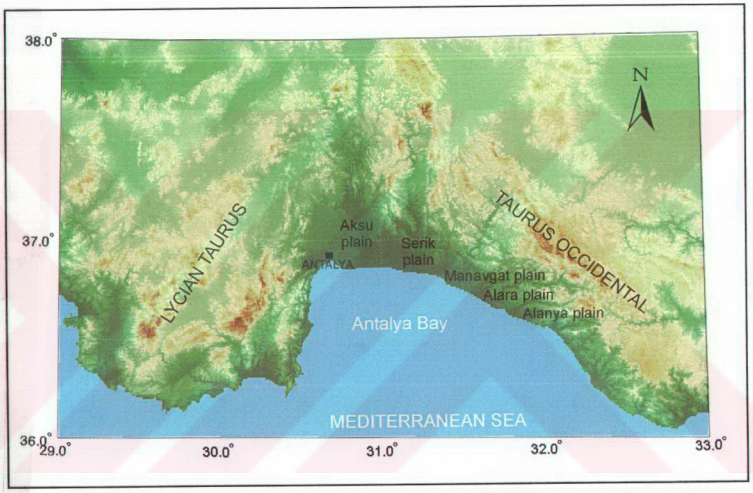

Figure 1.2 : Map showing the western part of the Taurids (modified from Blumenthal, 1947 and Brunn *et al.*, 1971).

In western part of the Antalya Bay, no wide coastal plain were developed in the coastal area because the closeness of the Lycian Taurus to the coast (Figure 1.2). However in the northern and eastern coasts of the Antalya Bay, as a result of the increasing of the distance between mountains and coastline (Evans, 1970), several coastal plains exist (Figure 1.2). The main coastal plains, occurring around the major rivers, are: Aksu, Serik, Manavgat, Alara and Alanya. These plains have been formed by alluvial succession of the rivers (Evans, 1970).

In Antalya Bay area, the most important rivers are Düden, Aksu, Köprüçay, Manavgat, Alara, and Dimçay rivers (Figure 1.3). These rivers play an important role in the formation of coastal plains (Evans, 1970). Moreover, there are many streams such as Ulupınar, Kocaçay, Kesme, Göynük, Acısu, Karpuz and Kargı streams, without a regular regime. The water levels of these small rivers (streams) decrease in summer months and increase from autumn to spring (Evans, 1970).

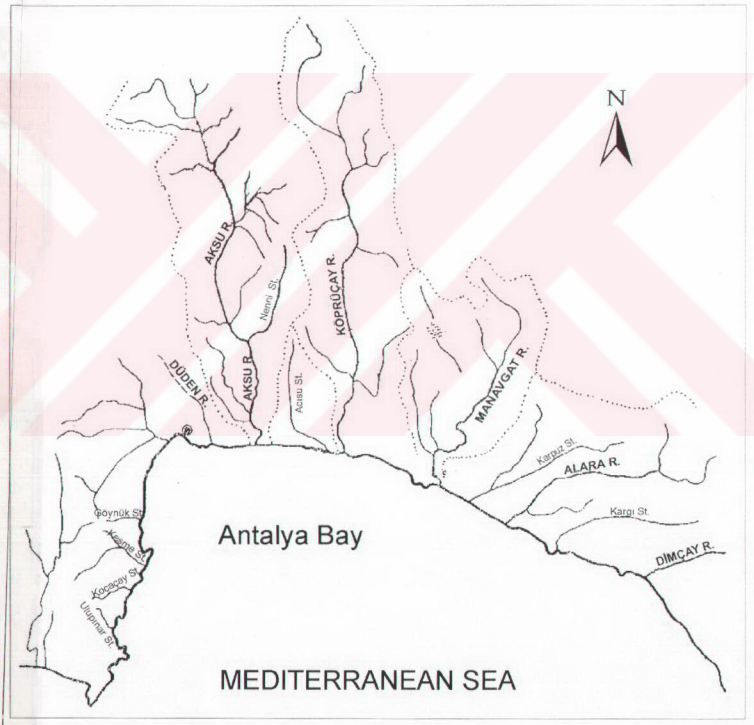

Figure 1.3: Map showing the rivers and their drainage areas on the coastal plain surrounding Antalya Bay (EİE, 1995).

Aksu River has a drainage area of 6472 km^2 with a long-term mean discharge of 1299 hm^3/year (EİE, 1995; Table 1.1). Köprüçay River drains a smaller area (1974 km^2) than Aksu River, but it has a discharge of 3090 hm^3/year (EİE, 1995; Table 1.1). Manavgat River has a drainage area of 1478 km^2 and its average discharge (4748 hm^3/year) is higher than the other rivers located in Antalya Bay (EİE, 1995; Table 1.1).

Table 1.1 : River and stream discharges into the Antalya Bay (compiled from EİE, 1995).

Rivers and Streams	Discharge (hm^3/year)
Düden R.	651
Aksu R.	1299
Köprüçay R.	3090
Manavgat R.	4748
Alara R.	990
Dimçay R.	509
Kargı St.	246
Karpuz St.	171
Sedre St.	135
Bıçkıcı St.	171
Others	1350

1.3 Climate

A Mediterranean climate dominates on the southern coast of Turkey. The characteristics of this climate are hot dry summers and mild wet winters (Evans, 1970). The annual mean temperature is 18.4° C for the years 1961-1995 (DSİ, 2000). Temperature reaches the maximum value (27.9 °C) in July and the minimum value (9.7 °C) in January (DSİ, 2000; Figure 1.4).

Figure 1.4 : Monthly mean temperature values between 1961-1995 (DSİ, 2000).

he annual mean precipitation is 1034.7 mm between the years 1931-1995 (DSİ, 2000). ienerally, the maximum rainfall values are observed (> 256 mm) in December, and the inimum rainfall values (< 4.3 mm) in August (DSİ, 2000; Figure 1.5).

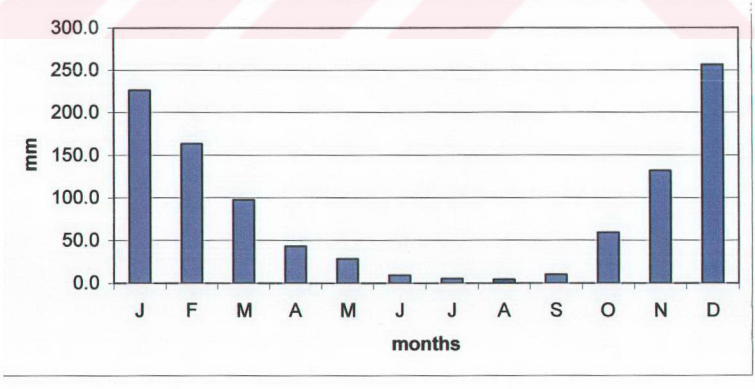

Figure 1.5 : Monthly mean precipitation values between 1931-1995 (DSİ, 2000).

1.4 Water masses and circulation patterns

In Mediterranean, the rate of evaporation is greater than the inflow from rain and rivers. The water budget is balanced by the water exchange between Mediterranean and Atlantic Ocean via Gibraltar Strait (Özsoy *et al.,* 1989; Malanotte-Rizzoli *et al.,* 1999).

The Levantine Basin is the second largest basin of the Eastern Mediterranean. The major troughs in the northern Levantine Sea are the Rhodes, Antalya, Cilicia and Latakia with water depths of 4000, 2500, 1000 and 1500 meters, respectively (Özsoy *et al.,* 1989; 1993)

Four main water masses exist in the NW Levantine Sea; first is the surface water (SW), second is the Modified Atlantic Water (MAW), which originates from the Atlantic Ocean and characterized by a salinity minimum, third is the Levantine Intermediate Water (LIW) which is the saltiest water mass of the Eastern Mediterranean and is generated in late winter in several areas of the Levantine Basin, and finally Eastern Mediterranean Deep Water (EMDW) which is colder and less saline than LIW (Ünlüata, 1986; Özsoy *et al.,* 1987; Hecht *et al.*, 1988; Theoaris *et al.,* 1993).

In summer, a thin layer, between the depths of 25 and 30 meters, is observed at the surface with a high salinity (39.1-39.3 ‰), due to high temperature and evaporation (Figure 1.6). Beneath this layer, MAW occurs with a thickness of 100 m (Figure 1.6). This Atlantic water has a low salinity (36.5-38.5 ‰) and low temperature (15° C). In winter, the presence of Atlantic Waters in the Levantine Sea is often reduced as a result of increased mixing (Özsoy *et al.,* 1989).

The Levantine Intermediate Water occupies the intermediate layers between the depths of 200 and 700 m (Figure 1.6). It is characterized by high salinity (39.1-39.3 ‰), and it is known to be formed in the Levantine Sea (Hecht *et al.*, 1988; Malanotte-Rizzoli *et al.,* 1999).

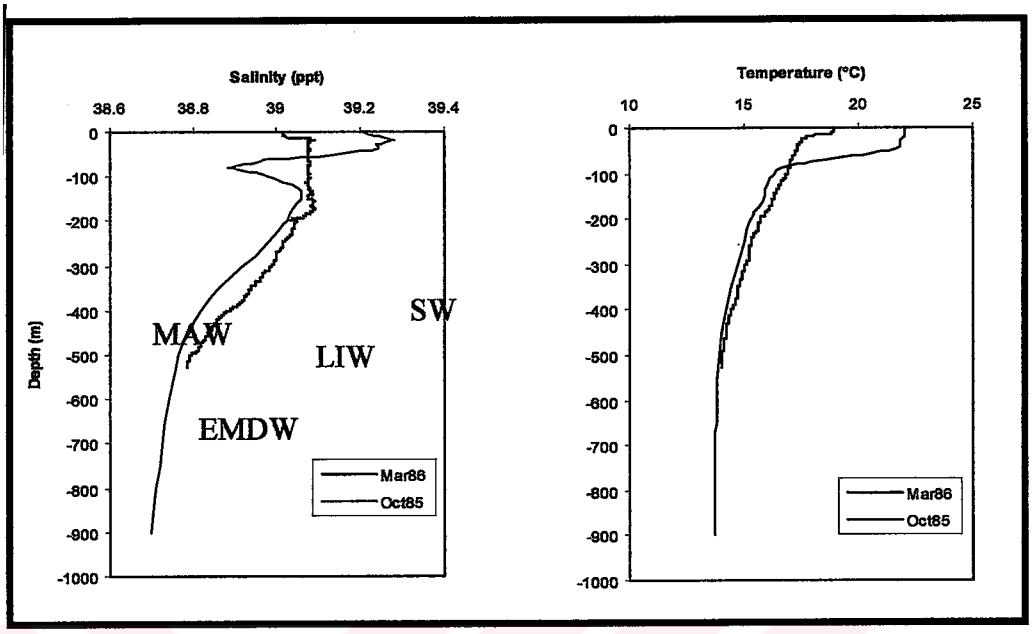

Figure 1.6 : General salinity and temperature profiles for summer and winter months (modified from Özsoy *et al.*, 1993).

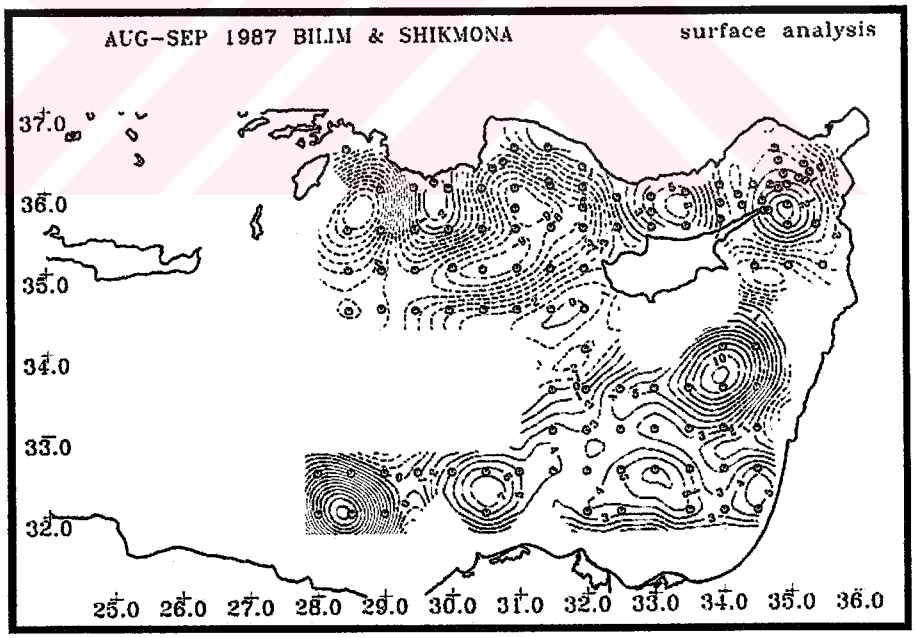

Figure 1.7 : Surface dynamic height (in cm) referenced to 800 decibar level of no motion, August-September 1987 (from Özsoy *et al.*, 1993).

From 700 m to deep waters, there is Eastern Mediterranean Deep Water that has low salinity and low temperature than LIW (Özsoy *et al.*, 1989; Malanotte-Rizzoli *et al.*, 1999).

In Eastern Mediterranean, circulation system is formed by a series of meso-scale eddies and the currents with different directions (Özsoy *et al.*, 1993; Figure 1.7).

The hydrological features consists of a series of dynamically interacting sub-basin scale eddies (the Rhodes cyclonic, Mersa Matruh anticyclonic and Shikmona anticyclonic gyres) and embedded coherent structures (the Anaximander, Antalya, Cilician and Ierapetra anticyclonic eddies) fed by bifurcating jet flows (the Mid-Mediterranean Current and Asia Minor Current, AMC) (Özsoy *et al.*, 1993; Figure 1.7).

1.5 Tectonic model for evolution of the study area

The onshore geologic units of the Antalya Bay constitute the southern regions of Isparta Angle (Figure 1.8). It is believed that the structural and tectonic history of the Isparta Angle has been initiated in Mesozoic with the rifting of the North African continent (Poisson, 1984; Robertson and Dixon, 1984; Şengör *et al.*, 1984). The seaways or oceanic basin formed in Mesozoic and closed during late Cretaceous- early Tertiary with culminating in final emplacement of Antalya Complex (Robertson, 1998).

Antalya Basin that has been produced in Messinian by extensional faulting, is a southward-widening rift basin that is interpreted as the results of crustal extension behind a subduction zone linking the Florence Rise with the southern boundary of the Anaximander Seamounts (Robertson, 1998). During the Miocene (Figure 1.9 A) a division clearly existed between a precollisional setting in the easternmost Mediterranean (west of the longitude of the Levant margin) and a collisional setting in southeastern Turkey. During this time, east-west compression affected the Aksu Basin further west. These events record were consequent upon collision in southeast Turkey, and the final stages of emplacement of the Lycian Nappes (Figure 1.9 B). In coastal

southern Turkey, regional uplift took place in late Pliocene-early Pleistocene time (Figure 1.9 C), associated with crustal extension faulting of the Aksu Basin (Robertson, 1998).

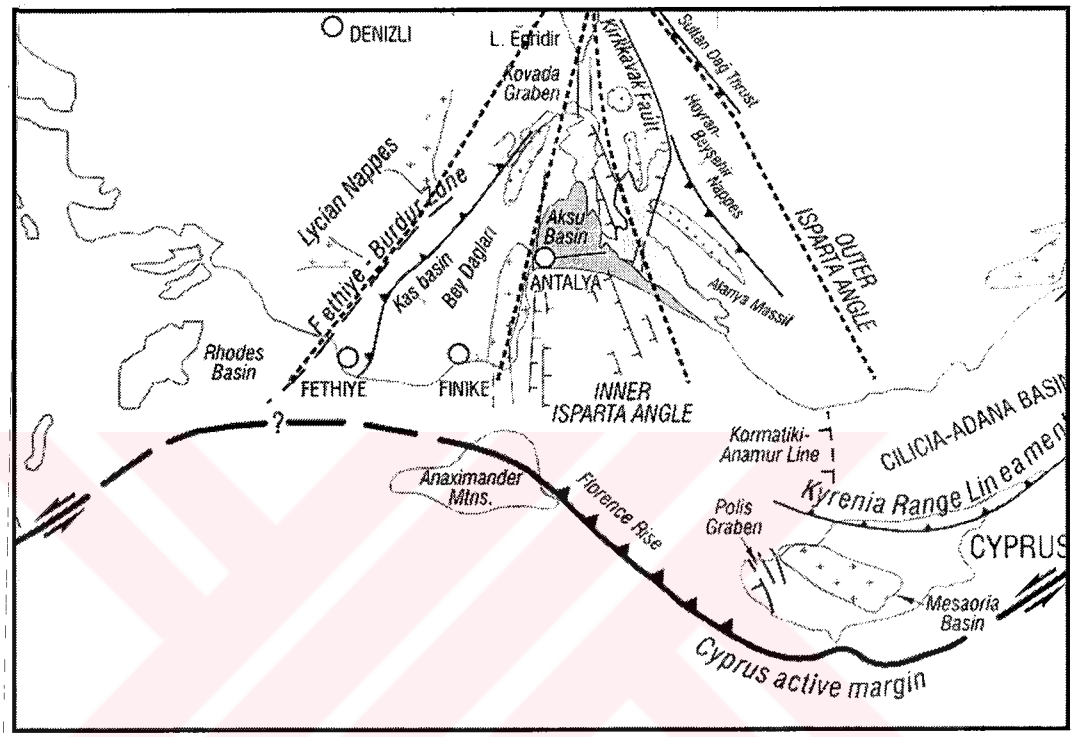

Figure 1.8: Outline tectonic map of the easternmost Mediterranean area showing the main lineaments and the main structural units and basins (modified from Glover and Robertson, 1998a).

According to Robertson (1998), during Pleistocene–Holocene times, existing plate boundaries were active. Northeastward subduction was active beneath southwest Cyprus and the southern Antalya Bay area. Crustal extension has continued onshore in the Antalya Basin (Robertson, 1998).

The western margin of the Antalya Bay is marked by a series of steep down-to-the east normal faults (Figure 1.8; Glover, 1996). The northeastern Antalya Bay is characterized by more widely spaced faults that locally define a horst and graben structure (Figure 1.8; Glover, 1996; Glover and Robertson 1998a).

1.6 Geological settings

The knowledge about the deep structure of Antalya Bay comes from a few seismic researches (Özhan 1988; Glover and Robertson, 1998a). According to Woodside (1977), the lowest layer in the sub seafloor of the eastern Mediterranean Sea, which is indicated by evaporites in seismic records, is a formation of pre-Messinian age (Figure 1.10).

Seismic data from Antalya Bay offshore from Aksu Basin also indicate that the marine Pliocene that overlay the Messinian evaporites, is approximately 500 meters thick and contains three transgressive events that can be probably be related to eustatic sea level changes (Glover and Robertson, 1998b).

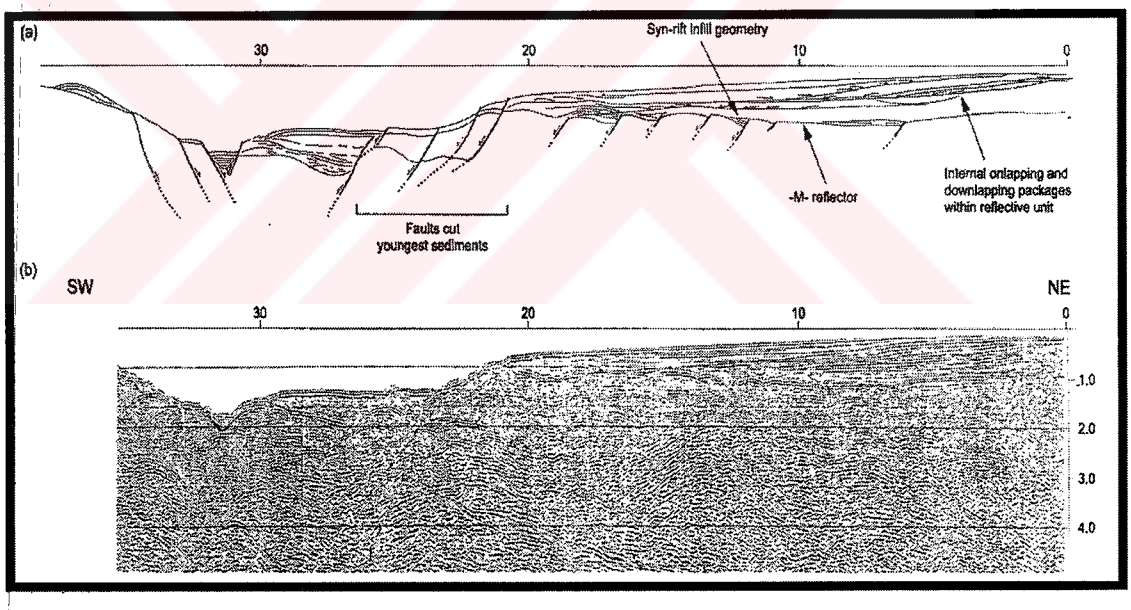

Figure 1.10 : Shallow reflection data taken from Antalya Bay. (a) Line interpretation. Note the presence of an inferred strong Messinian reflector (-M-), that is block faulted and overlain by inferred Pliocene sediments. (b) Uninterpreted seismic data (from Glover and Robertson, 1998a).

The onshore Antalya Bay is composed of three distinct main geological regions, which take parts in the Isparta Angle. The Isparta Angle is a triangular-shape region that

separates the western and the central Tauride Mountains, and extends offshore into Antalya Bay (Glover and Robertson, 1998a).

The coastal regions, from west to east, are: Antalya Complex, Aksu Basin and Alanya Massif (Figure 1.11; Glover and Robertson, 1998a).

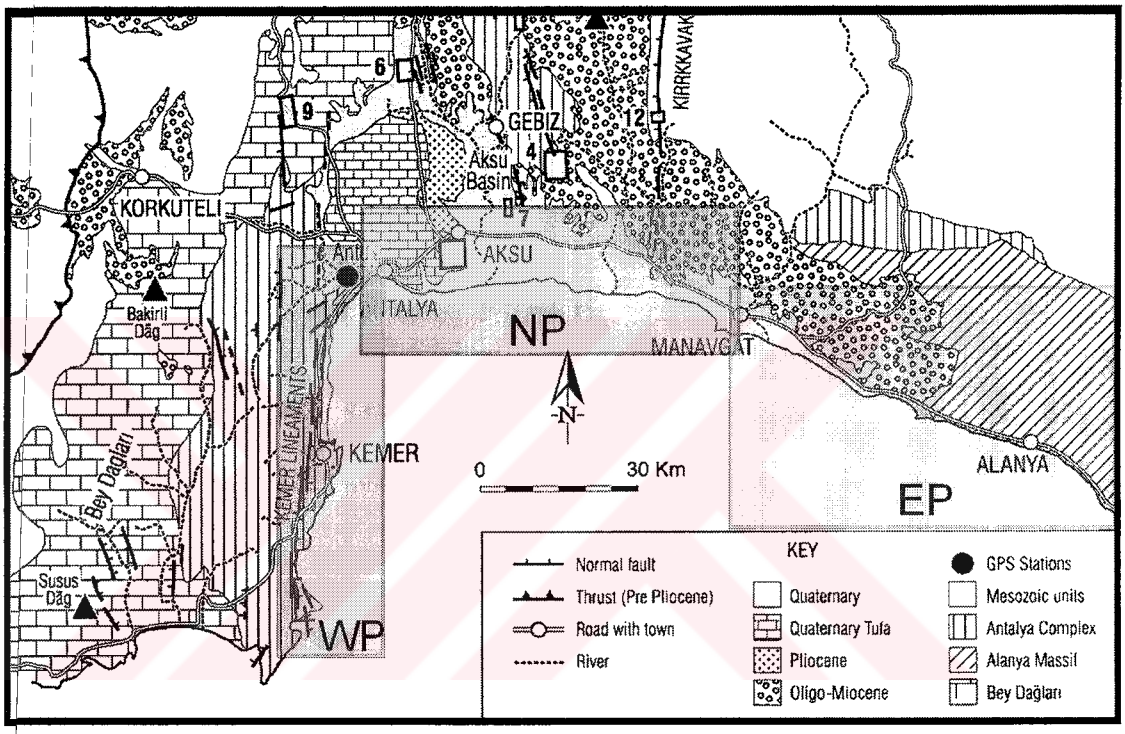

Figure 1.11 : Geological map showing the main stratigraphic units of the area, and the main neotectonic lineaments (modified from Glover and Robertson, 1998a). WP is western region, NP is northern region and EP is eastern region (see text for detailed explanation).

Antalya Complex

The Antalya Complex has a regional northward-pointing V-shaped outcrop pattern, defining the Isparta Angle (Figure 1.11; Robertson, 1998). The Antalya Complex is divided into a number of segments exposed in different parts of the Isparta Angle (Robertson, 1993). The adjacent area to Antalya Bay corresponds to the SW segment of the Antalya Complex, and it includes Mesozoic carbonate platform, deep water

sediments of Late Triassic to late Cretaceous age and ophiolitic rocks that record the formation and tectonic emplacement of a small Mesozoic ocean basin (Robertson and Woodcock, 1984).

There are two different views on the geology and tectonic formation of the SW Antalya Complex. According to some investigators (Brunn, 1974; Monod, 1976; Ricou *et al.*, 1974; 1975; Delaune-Mayere *et al.,* 1977) the evolution of the SW Antalya Complex is related to three nappes; Tahtalı Dağ carbonates, Alakırçay nappe and Bey Dağları unit.

However, Robertson and Woodcock (1981) explained the present assemblage of SW Antalya Complex as a passive Mesozoic margin of a south-Tethyan oceanic basin separating into five zones (Figure 1.12). These zones are, from west to east, Bey Dağları, Kumluca, Gödene, Kemer and Tekirova (Figure 1.12; Robertson and Woodcock, 1981). These are explained below:

- Bey Dağları Zone is interpreted as relatively autochthonous massif Mesozoic carbonate platform that locally is overlain by Miocene foreland basin clastic sediments (Figure 1.12).
- The Kumluca Zone is described as the deformed deep-water, southeasterly passive margin of the Bey Dağları carbonate platform to the west (Figure 1.12).
- The Gödene Zone is interpreted as relatively proximal oceanic crust, and both shallow and deep water sedimentary units (Figure 1.12).
- The Kemer Zone is viewed as several, slivers of continental crust that were rifted from the larger Bey Dağları continental fragment in the Triassic (Figure 1.12).
- The Tekirova Zone is interpreted as oceanic crust and mantle of late cretaceous age formed within the southerly Neotethys oceanic basin. This zone is a major ophiolite complex exposed along the present coast (Figure 1.12).

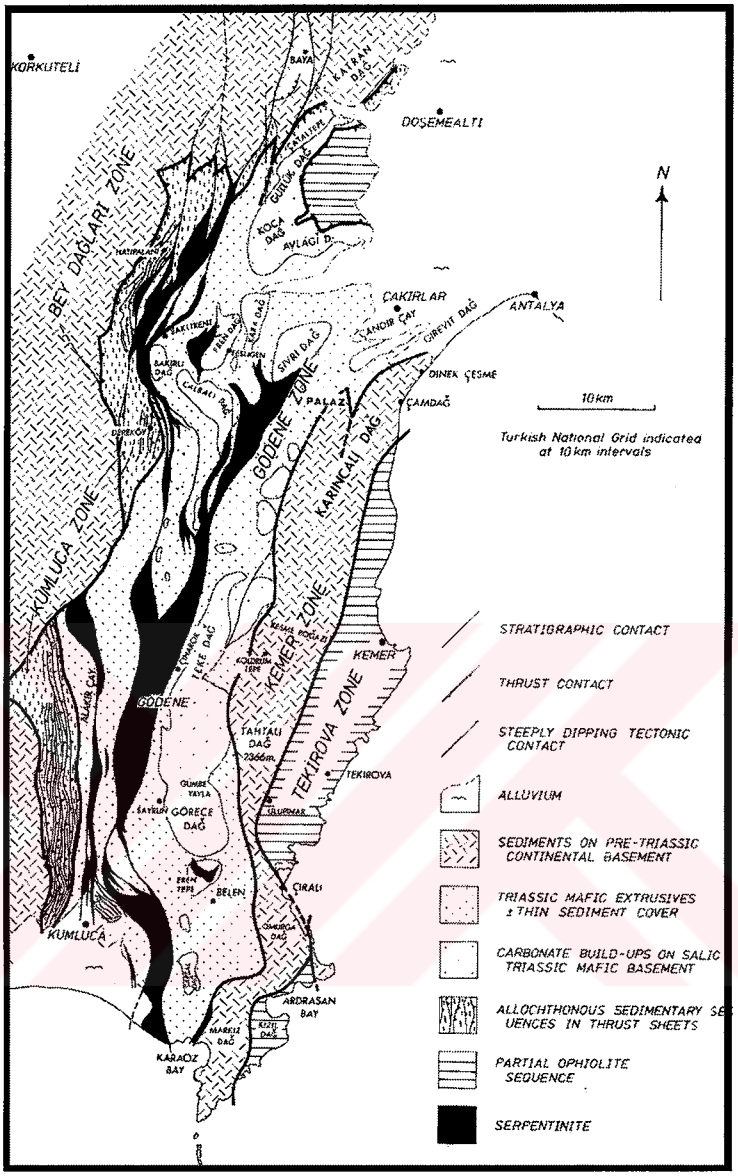

Figure 1.12 : Simplified geological map showing the main lithologies and tectonic notation of the SW Antalya Complex (from Robertson and Woodcock, 1981).

Aksu Basin

The Pliocene-Pleistocene Aksu Basin (Figure 1.11) is interpreted in terms of an initial late Miocene transtensional rift event, followed by an early to mid-Pliocene sedimentary infill, followed by further rifting and extension in the latest Pliocene-early Pleistocene

that was associated with uplift of the adjacent Taurus Mountains (Glover and Robertson, 1993; Glover and Robertson, 1998b).

Pleistocene in Aksu Basin is characterized by extensive tufa deposits ("Antalya Travertine"; Bürger, 1990) that precipitated from cool-water spring are observed. The Antalya travertine occurs on a thin (tens of meters) late Pliocene to early Holocene alluvial succession (Glover, 1996). Beneath this, a Messinian to mid-Pliocene extensional basin is in filled with shallow-marine to deltaic sediments up to several hundred meters thick (Glover, 1996). The onshore Pliocene-Pleistocene succession rests unconformably on older sediments of the Miocene Aksu Basin (Akay *et al.,* 1985).

Alanya Massif

The Alanya Massif (Figure 1.11) is the name given to a large area of metamorphic rocks situated east of Antalya Bay (Blumenthal 1951). The Alanya Massif is located at the east of Antalya Bay, forming the coastline between Anamur and Manavgat. Alanya Massif consists of three superposed, relatively flat-lying, crystalline nappes "Alanya Nappes" (Okay and Özgül, 1984). From bottom to top these nappes are explained below:

Mahmutlar Nappe consists of a heterogeneous series of shales, sandstones, dolomites, limestones and quartzites (Okay and Özgül, 1984). Sugözü Nappe is made up of garnet-micaschists which contain bands and lenses of eclogites and blueachist metabasites (Okay and Özgül, 1984). Yumrudağ Nappe, consists of a thick Permian carbonate sequence underlain by a relatively thin schist unit (Okay and Özgül, 1984). These three nappes overlie the predominantly Mesozoic continental margin type lithologies of the Antalya Complex. The rocks belonging to the Antalya Complex outcrop beneath these nappes in a large tectonic window (Okay and Özgül, 1984).

In the Manavgat area, Alanya Massif is unconformably overlain by Miocene-Lower Pliocene marine sediments of the Manavgat Basin (Akay *et al.,* 1985; Flecker *et al.,* 1995). The highest part of the preserved succession is made up of open-marine muddy

sediments of early Pliocene age (Glover and Robertson, 1998b). The Manavgat Basin reflects a phase of initial, early Miocene northward marine transgression over the metamorphic Alanya Massif, followed by abrupt subsidence that marks the start of in Mid-Miocene deeper-water deposition (Robertson, 1998).

On a regional scale, the Manavgat Basin could be interpreted either as an extensional basin dating from the early Miocene, or as a flexural foreland basin related to generally southward thrusting of units in the Taurus Mountains to the north (Robertson, 1998).

1.7 Quaternary sea level changes

Sea level changes have been played important roles on the evolution of the coast and the continental margins. Changes of sea level were largely the result of several interacting isostatic, eustatic and geoidal processes (Erinç, 1963; King 1972; Komar, 1976; Vail *et al.,* 1977; Bowen, 1978; Kennett, 1982). Of these processes, eustatic sea level change is more important than the others.

The eustatic sea level change acts on global scale and occurs as a result of a change in the total volume of ocean basin or a change in the volume of seawater. Four kinds of eustatic effects exist:

- Tectono-eustatic that is related to tectonic activities in oceans
- Sedimento-eustatic that is related to sediment accumulation in ocean basin
- Glacio-eustatic that is result of the changes in global ice volume
- Addition of juvenile water from submarine volcanism

Today, it is widely believed that the Quaternary sea level changes are mainly caused by glacio-eustatism (King, 1972; Shepard, 1973; Komar, 1976; Bowen, 1978; Kennett, 1982). The formation of the ice sheets during glacial ages and the melting of these sheets during interglacial times cause great oscillations in sea level through the Quaternary times. The amplitude of these oscillations is believed to have been at least 130 m and possibly considerable more (Emiliani and Flint, 1980).

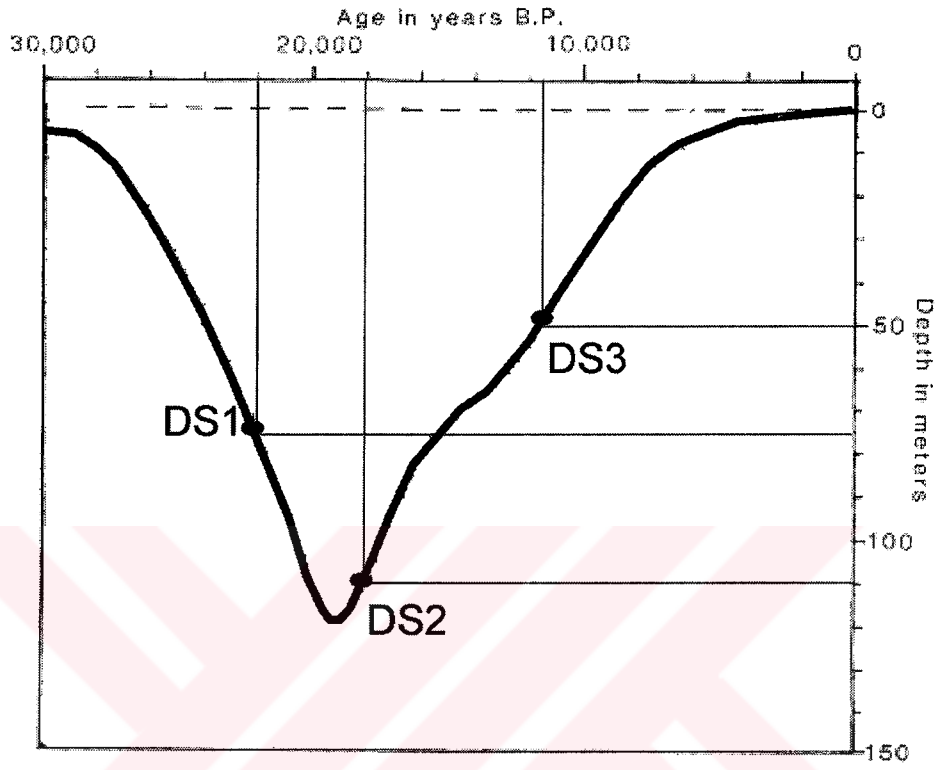

Figure 1.13: Sea level changes during the last 30 000 yrs for the eastern Mediterranean (Arbouille and Stanley, 1991). DS1, DS2 and DS3 indicates the pinch out position of the depositional sequence 1, 2 and 3 respectively (for explanation see text).

t is explained that the last glacial age started about 75 ka B.P. and reached the naximum 18 to 20 ka B.P., (Curray, 1961, 1964; Morner, 1971; King, 1972; Herman, 1972; Kennett, 1982). At that time the sea level was about 130 m below the present sea evel (Fairbanks, 1989). This is the lowest sea level during the Quaternary (Curray, 1964; Milliman and Emery, 1968; Kennett, 1982). Following the last glacial maximum he climate entered a warming trend and a rise in sea level ("Holocene" or "Flandrian" ransgression) has been initiated (Curray, 1964).

The chronology of sea level change over the past 30 000 years, for the eastern Mediterranean, is shown in Figure 1.13. It seems that the sea level was below 15 m from

the present level, at about 30 000 years ago (Figure 1.13). From that time towards to the 20 000 years ago, a continuous lowering of the sea level took place down to 120 m depth, being the reference point of the initiation of the Holocene transgression. For that time to present rising of the sea level is observed (Figure 1.13). It has been concluded that the sea level reached to its present position approximately 3 000 years ago (Curray, 1964).

1.8 Objective of the study

The onshore geology of the Antalya Bay with complex structure arouses interest of many scientists (Evans, 1970; Brunn *et al.,* 1971; Robertson and Woodcock, 1984; Waldron, 1984; Hayward, 1984; Reuber; 1984; Yılmaz, 1984; Okay and Özgül, 1984; Akay *et al.,* 1985; Pentecost, 1995; Glover, 1996; Flecker *et al.,* 1998; Glover and Robertson, 1998a, 1998b; Robertson, 1998). In spite of these abundant investigations on land, limited number of offshore geological and geophysical surveys have been carried out on the Antalya Bay. Structure and evolution of Antalya Basin have been studied by Woodside (1977), Özhan (1988), and Glover and Robertson (1998a). Salt related deformations in the deep Antalya Basin have also been investigated by Taviani and Rossi (1989).

This study aims to investigate the seismic stratigraphy of the continental shelf of the Antalya Bay to explain the distribution pattern of late Quaternary sediments using bathymetric and high-resolution seismic data. No previous seismic study of this type has been carried out in the Antalya Bay.

CHAPTER TWO
MATERIAL AND METHODS

2.1 Source of data

The data used in this study were collected during the cruise of TÜBİTAK Project (199Y074) in 1999, using R/V Bilim of the Institute of Marine Sciences / METU.

2.2 Position fixing

A Trimble NT200 Global Positioning System (GPS) was used to fix the position of the vessel during the study. This system is basically consisted of a Control Display Unit (CDU), a graphic display and a six-channel GPS receiver. It has also a Smart Card Reader (SCR) that provides a real-time imaging of survey vessels on a nautical chart. Trimble NT200 GPS works with 12/24 VDC. Its positional accuracy in differential mode is about ±20 meters.

2.3 Depth recording

During the survey, the depth values were taken by JMC F-830 echo sounder system that is mounted to the research vessel, R/V Bilim. This echo sounder system enables to record depth values both analogue and digital. It produces graph recording using thermal paper. The system has two transducers operating frequencies of 38 and 200 kHz. In this study, 200 kHz frequencies were used. The maximum depth measuring range of the echo sounder is 2600 meters.

The system works simultaneously with GPS system to determine the depth value of a point with accurate coordinates.

The depth records taken along the each survey lines (Appendix 1) were used to prepare the bathymetric map of the area. The depths reading at each position fixes were

transferred to a map. Following this procedure, a bathymetric map of the area was produced (Appendix 2) by using the Surfer graphical package (Golden Software, Inc., Colorado, USA). Nearshore areas were contoured at 10 meters intervals up to 20 meters. The areas within the depths of 20 and 200 meters were drawn at 20 meters interval. Additionally, some depth values among the survey lines were supplemented from the Turkish Navy Charts (1970, 1974, 1975, 1976). The bathymetric map presented in this study includes 1501 data values on depth readings.

2.4 Sub-bottom profiling

To investigate the sub-bottom geology of the study area, an EG&G Uniboom high-resolution reflection-profiling system was used.

This single channel seismic system consists of a recorder (Model 255), an energy source (Model 234), a single plate Uniboom sound source (Model 230-1) and eight-element hydrophone (Model 265).

The most important feature of this system is the capability of separating the reflectors very close to one another, and this peculiarity is referred to as high-resolution. Its broad frequency spectrum (400 Hz-14 kHz) enables the resolution of about 15-30 cm. The Uniboom system, having a broad frequency spectrum, provides a low penetration of sub bottom layers to a depth of 75 meters.

In the present study, continuous seismic profiles were collected along approximately 265 km of track lines (Appendix 1). Of a total of 56 cruise lines; six of them were run parallel to the shore, whilst the remaining surveys were carried out normal to shore (Appendix 1).

Depth conversions from time sections on seismic data were made using a sound velocity of 1500 m/s for water and 1700 m/s for sediments (cf. Malovitsky *et al.,* 1975; Okyar, 1991; Ergin *et al.,* 1992; Ediger *et al.,* 1993; Tezcan and Okyar, 2001).

2.5 Seismic stratigraphy

Seismic data obtained from this study were interpreted by using the principles of seismic stratigraphy method (Mitchum *et al.,* 1977a, 1977b; Sangree and Widmier, 1977, 1979; Vail *et al.,* 1977; Brown and Fisher, 1977, 1980; Badley, 1985; Boggs, 1987; Macdonald, 1991).

This method has been applied to high-resolution seismic profiles from shelf areas in the Mediterranean Sea by a number of investigators (e.g., Stefanon, 1985; Got *et al.,* 1987, Canals *et al.,* 1988; Okyar, 1991; Aksu *et al.,* 1992; Ergin *et al.,* 1992; Ediger *et al.,* 1993; Tezcan and Okyar, 2001).

Seismic stratigraphy is a geologic approach to the stratigraphic interpretation of seismic data. Seismic reflection terminations and configurations are interpreted as stratification patterns, and are used for recognition and correlation of depositional sequences, interpretation of depositional environment, and estimations of lithofacies.

The procedure used for seismic stratigraphic method comprises two main analyses:

- Seismic sequence analysis
- Seismic facies analysis

2.5.1 Seismic sequence analysis

Seismic sequence analysis is utilised to recognize the depositional sequence by dividing the seismic section into sequences. Depositional sequence is defined as a stratigraphic unit composed of a relatively conformable succession of genetically related strata bounded by unconformities or their correlative conformities (Mitchum *et al.,* 1977a). On seismic profiles, regional unconformities could be identified through the physical relationship of strata to upper and lower boundaries of a sequence (Figure 2.1).

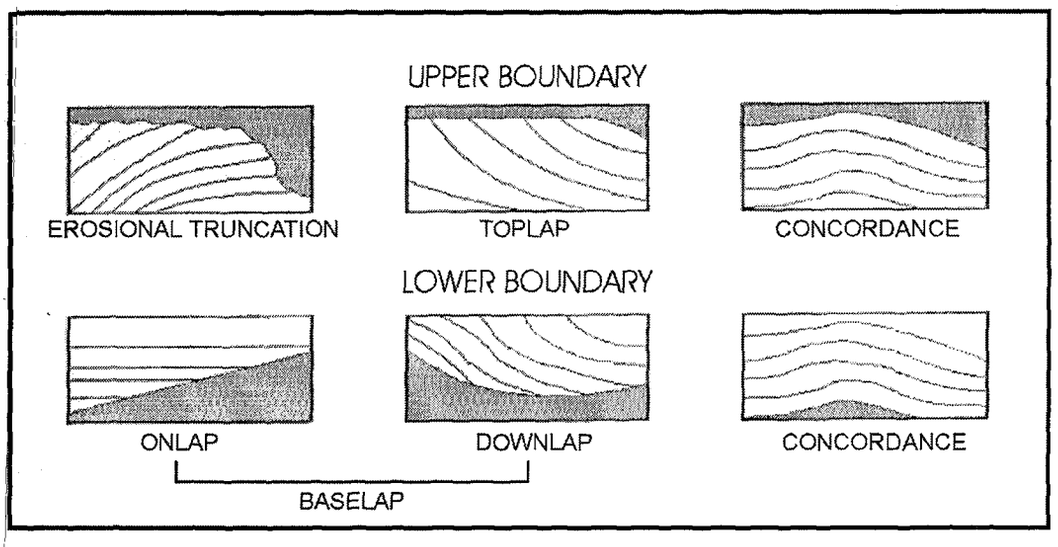

Figure 2.1 : Relationships between strata boundaries and depositional sequences (from Mitchum *et al.*, 1977a).

2.5.2 Seismic facies analysis

By combining the analysis of stratal relationships with the attributes of individual reflection, it is often possible to obtain a detailed picture of the subsurface geology.

Seismic facies analysis is the description and geologic interpretation of seismic reflections parameters, including configuration, continuity, amplitude, frequency, and interval velocity (Table 2.1; Mitchum *et al.*, 1977b). Except for interval velocity and external geometry, these parameters can be evaluated visually on the seismic data. After seismic facies units are recognized, their limits defined, and areal association mapped, they are interpreted to express stratification, lithologic and depositional feature of the deposits.

Table 2.1: Seismic reflection parameters used in seismic stratigraphy and their geologic significance (after Mitchum *et al.*, 1977b).

Seismic facies parameters	Geologic interpretation
Reflection configuration	▪ Bedding patterns ▪ Depositional processes ▪ Erosion and paleotopography ▪ Fluid contacts
Reflection continuity	▪ Bedding continuity ▪ Depositional processes
Reflection amplitude	▪ Velocity-density contrast ▪ Bed spacing ▪ Fluid content
Reflection frequency	▪ Bed thickness ▪ Fluid content
Internal velocity	▪ Estimation of lithology ▪ Estimation of porosity ▪ Fluid content
External form and areal association of seismic facies units	▪ Gross depositional environment ▪ Sediment source ▪ Geologic setting

Major groups of reflection configurations include parallel, divergent, prograding and chaotic patterns (Figure 2.2; Mitchum *et al.*, 1977b). *Parallel* patterns, including subparallel and wavy patterns are generated by strata that were probably deposited at uniform rates on a uniformly subsiding shelf or in a stable basin. *Divergent* configurations suggest lateral variations in rate of deposition or progressive tilting of the sedimentary surface during the deposition. *Prograding reflection* configurations include sigmoid, oblique and hummocky patterns. Prograding patterns are generated by the lateral outbuilding or prograding of strata. *Chaotic* reflection patterns represent a disordered arrangement of reflection surfaces owing to penecontemporaneous soft-sediment deformation, or possibly to deposition of strata in a variable, high-energy environment (Mitchum *et al.*, 1977b).

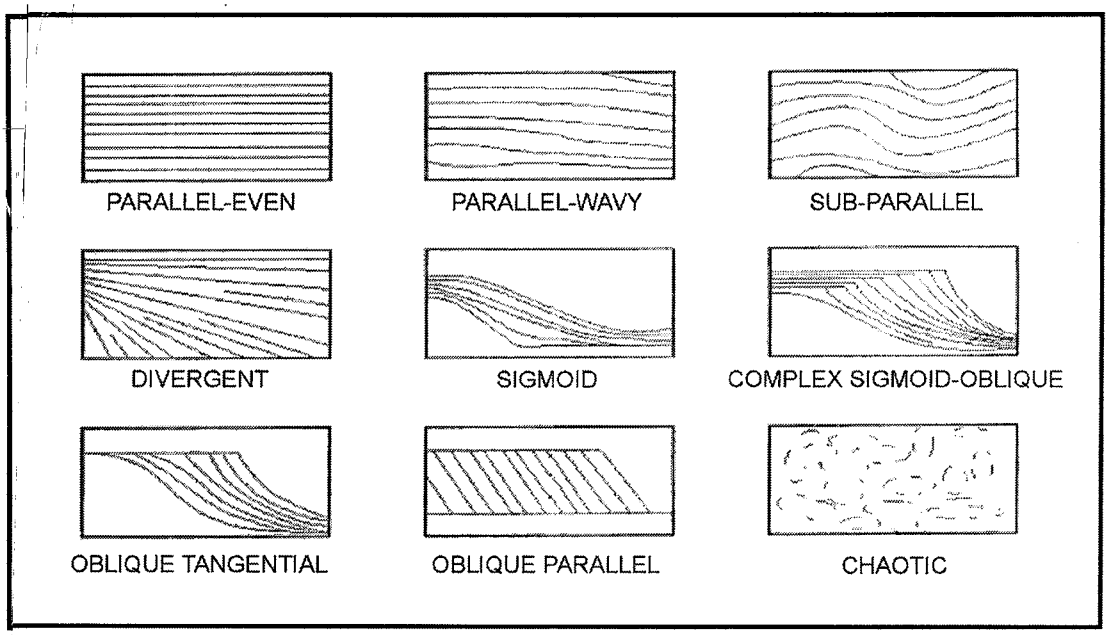

Figure 2.2 : Parallel-even, parallel-wavy, sub-parallel, divergent, sigmoid, complex sigmoid-oblique, oblique tangential, oblique parallel and chaotic seismic reflection configurations. Note, sigmoid, complex sigmoid oblique, oblique tangential, oblique parallel seismic reflection patterns are interpreted as prograding clinoforms (Mitchum et al., 1977b).

External forms of seismic facies units include sheet, sheet drape, wedge, bank, lens, mound and fill forms (Figure 2.3). Seismic facies units are interpreted in terms of the depositional environment, the energy of the depositing medium, and the lithologic content of the strata generating the seismic facies reflection pattern (Mitchum *et al.*, 1977b).

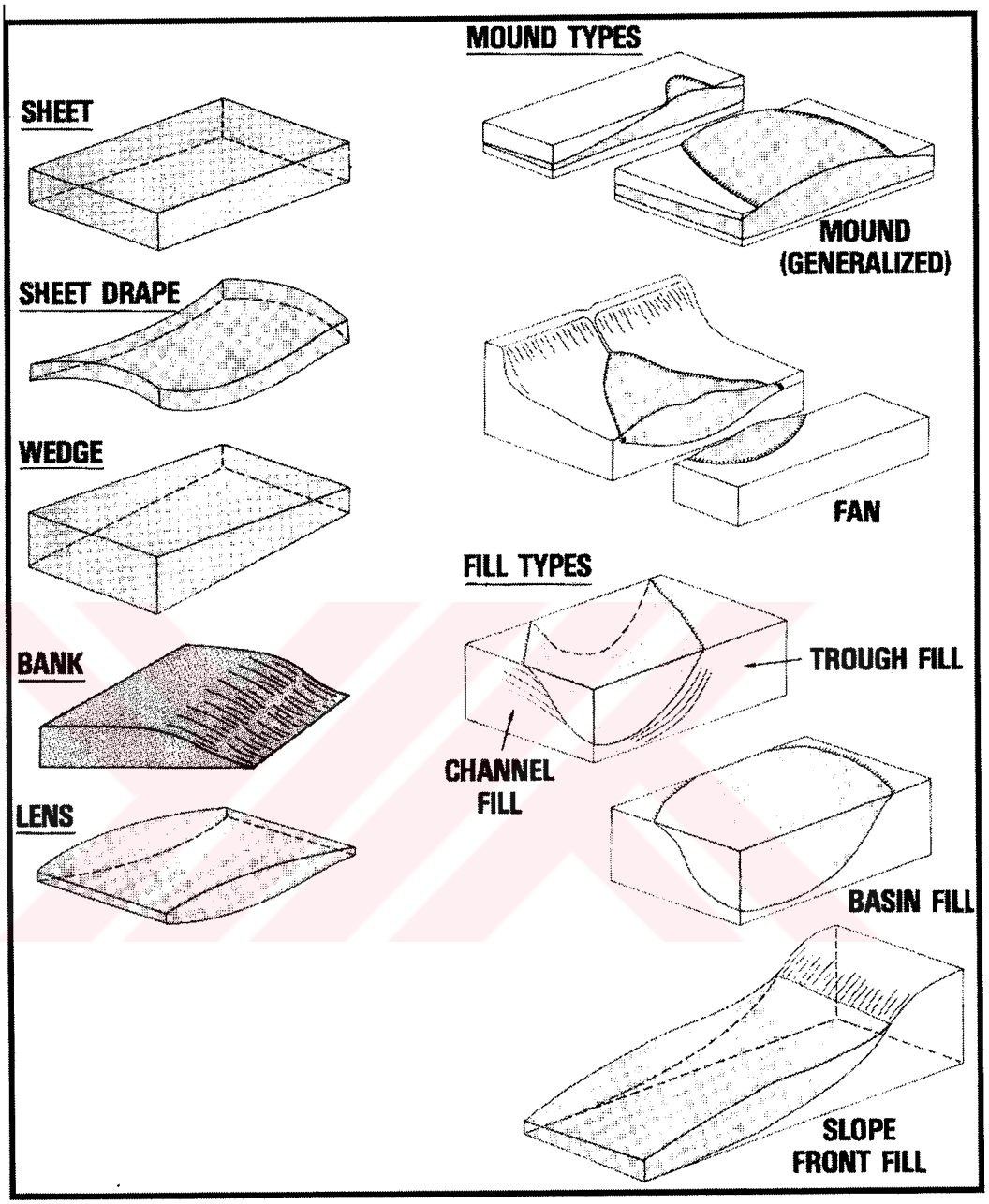

Figure 2.3: External forms of some seismic facies units (from Mitchum et al., 1977b).

CHAPTER THREE
INTERPRETATION OF DATA

3.1 Bathymetry and bottom features

For convenience, bathymetry and bottom features of the investigated area are separated into three distinct regions so as to compare them with the onshore geological setting of the Antalya Bay (Figure 1.11).

The western region

The western region is bordered between the offshore Cape Taşlık and Antalya, extending to a sea floor depth of 200 meters (Appendix 2). Landward, this region corresponds to the Antalya Complex (Figure 1.11).

Along the Cape Taşlık and Tekirova coasts, the shelf exceeds to the water depth of 200 meters (Appendix 2). This feature possibly indicates great amounts of sediment supply to the shelf area from the rivers on the coast (Appendix 2).

Towards the Antalya from the north of the Tekirova the shelf edge (transition from shelf to slope) is generally delineated by the 100 m isobaths (Appendix 2). The shelf area slopes gently, with an average gradient of 1.2°. However, off the Hurmaköy and north of Göynük, the shelf and slope are deeply dissected by two submarine canyons (Appendix 2; Tezcan and Okyar, 2001). The submarine canyon locating off the Hurmaköy can be of sedimentary origin, due to its proximity to the Göksu River mouth (Appendix 2). In the vicinity of other canyon (north of Göynük), no river and/or river channels are present that extend across the coast (Appendix 2). Therefore, its origin can be ascribed to tectonic processes.

The detailed interpretations of the echo-sounding records have revealed the presence of some irregular bottom features in the western shelf region (see Figure 3.1). These irregularities are possibly caused by the occurrences of barrier or ridge-like features. The echo character of the sounding profile resembles the current controlled erosional feature that has been described by many workers (Damuth, 1980; Klaus and Ledbetter, 1988; Okyar, 1991; Tezcan and Okyar, 2001).

Apart from this, some topographic irregularities are also found on the steep slope of the basin (Figure 3.2). Several modes of origin can be ascribed to these irregularities: slumping, faulting and formation by bottom-currents (e.g. Roos *et al.,* 1974).

The northern region

This region takes place between the offshore Antalya and Manavgat. Seaward, it is bordered by 200 m isobaths (Appendix 2). Onshore, this region is characterized by thick cover of Neogene and Holocene sediments (Figure 1.11).

In this region, shelf exceeds to the depth of 200 m, except off the Düden River mouth and off the Selimiye – Güzelbağ coasts (Appendix 2). The widening of the shelf is possibly related to high sediment input from the Aksu and Köprüçay rivers (Appendix 2). In general, the isobath contours along the shelf run in a W-E direction (Appendix 2). However, some small deviations are observed within general trend of the isobath contours, particularly off the Belekköy – Perakende coasts (Appendix 2). Here, the isobaths contours at the depths of 20 to 200 m exhibit an undulated appearance (Appendix 2), which may have been formed by faulting processes.

Off the Duden River mouth, sea floor is incised by a submarine canyon (Appendix 2). In the remainder sea floor area, off the Selimiye – Güzelbağ coasts, the shelf edge is delineated by the 100 m isobath (Appendix 2).

The echo-sounding records from the northern region imply the existence of some bottom irregularities (Figures 3.3-3.4). Of these, block like feature identified on echo sounding record (Figure 3.3) indicate the slumping processes in the canyon area (e.g. Damuth, 1980). The other irregularities seen on echo-sounding record (Figure 3.4) may be erosional features formed by bottom currents (e.g. Damuth, 1980;Klaus and Ledbetter, 1988; Okyar, 1991).

The eastern region

This region extends from the coasts of Manavgat and Gazipaşa to a depth of 200 meters (Appendix 2). On shore, this region takes a place between Manavgat and Alanya Massif (Figure 1.11). Off the river mouths (Karpuz, Alara, Kargı, Güz, Sapa and Paşa Rivers), the shelf is delineated by the 100 m isobath contour (Appendix 2). Here the shelf is about 4 to 6 km wide (Appendix 2). However in some areas, those seaward of Alanya and northwest of Gazipaşa (Appendix 2), the shelf is very narrow (< 0.5 km). These areas are characterized by canyon type morphology.

Sea floor of the eastern region exhibits some irregularities (Figures 3.5-3.6). For example, echo-sounding record obtained from the nearshore area of Mahmutlar explains the erosional effect of Dimçay River on the sea floor (Figure 3.5). Additionally, some small scale irregularities are observed on the sea floor close to the coast of Kargıcak-Alonçam (Figure 3.6). There may be two possible explanations of these irregularities. First explanation is that the observed irregularities may represent the presence of sand waves (e.g., Okyar and Ediger, 1997). An alternative interpretation is that the observed irregularities may be caused by the sea grass, such as *Posidonia Oceanica* (e.g., Ediger, 1987).

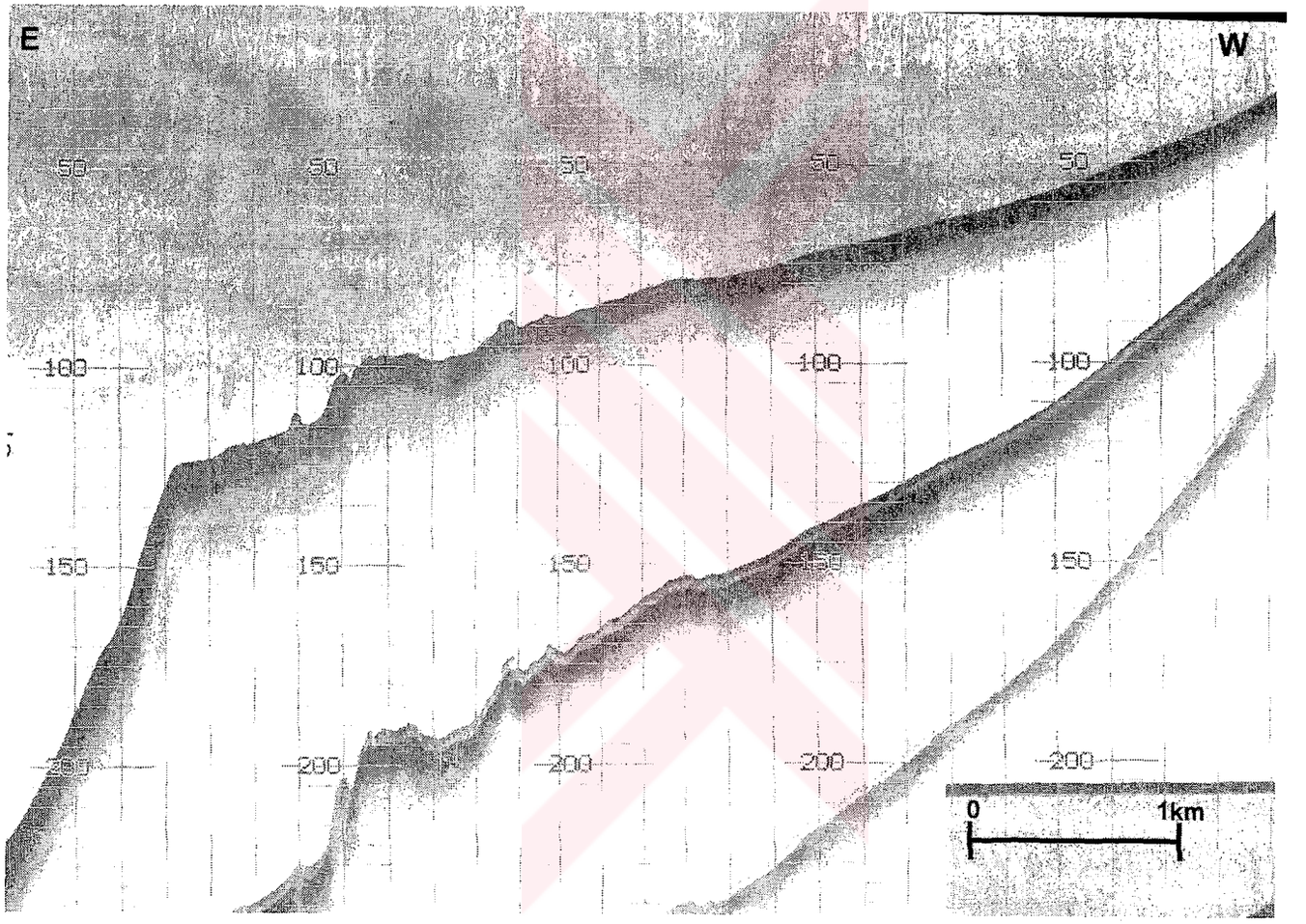

Figure 3.1: Echo-sounding profile showing some irregular features in the western shelf region (for location see Appendix 1).

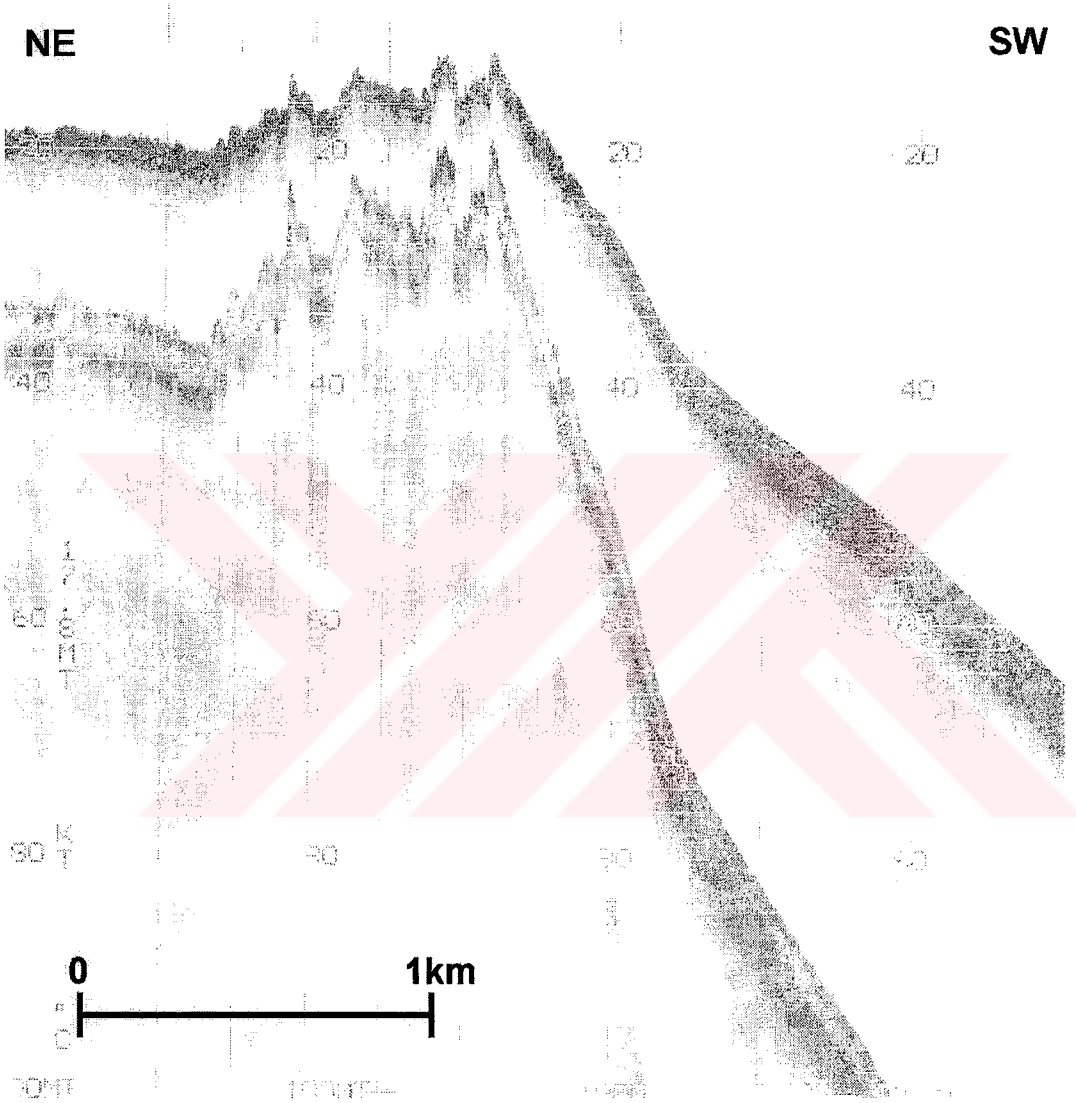

Figure 3.4: Echo-sounding profile showing current-contolled erosional features in the northern shelf region (for location see Appendix 1).

Figure 3.5: Echo sounding profile showing the erosional feature in the eastern shelf region. This feature is though to be formed by river flow (for location see Appendix 1).

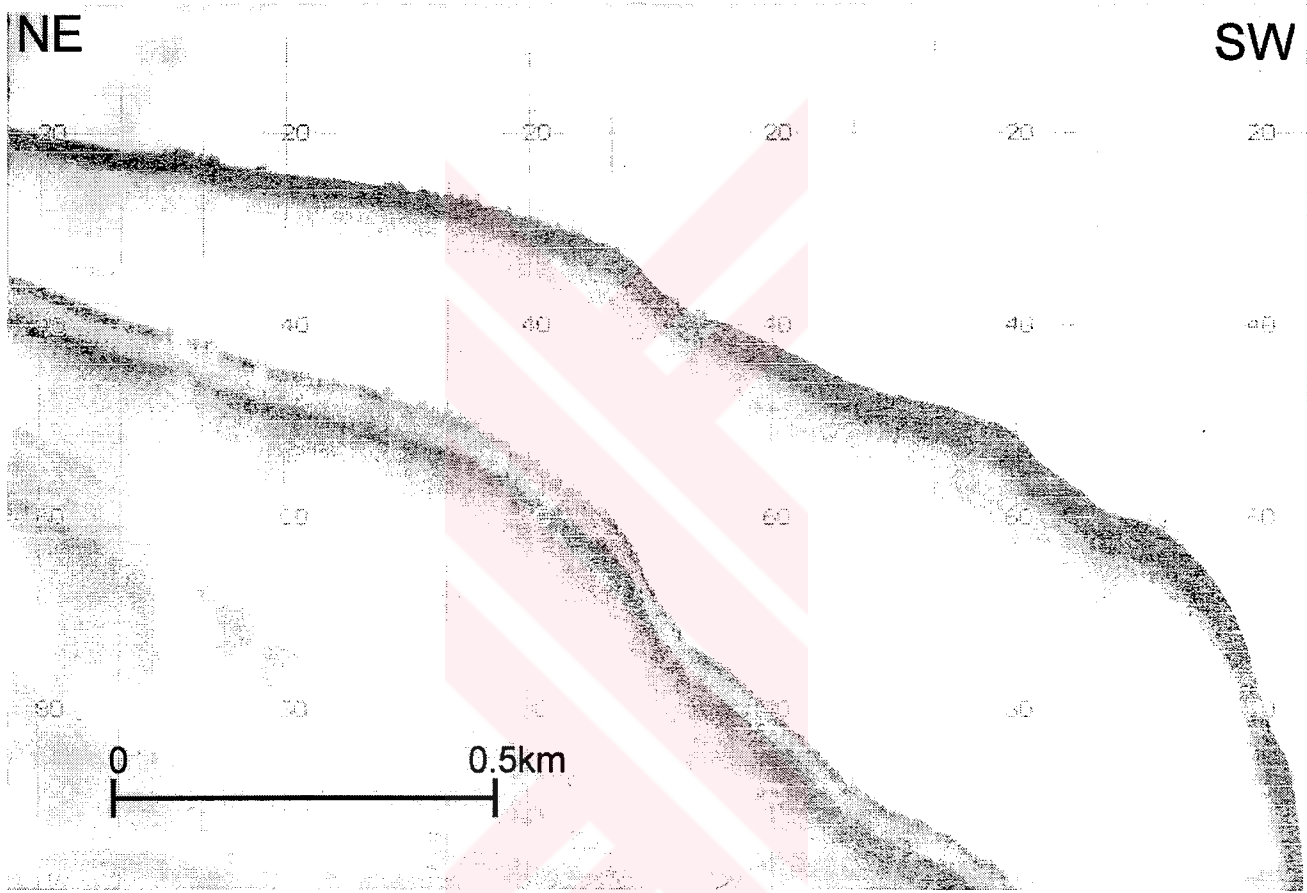

Figure 3.6: Echo-sounding profile showing some irregular features (sand waves and/or sea grass) in the eastern shelf region (for location see Appendix 1).

3.2 Sub-bottom stratigraphy

On the basis of the seismic stratigraphic analysis, four distinct depositional sequences overlying the acoustic basement (AB) have been identified in the surveyed area.

In descending order, these sequences are numbered as 1, 2, 3 and 4 (Appendices 7-21). Of these, the first sequence (1) is believed to have been deposited before the onset of the Holocene transgression "Flandrian transgression", whereas the last three sequences (2, 3 and 4) were deposited during the Holocene transgression (Tezcan and Okyar, 2001).

The boundary between Holocene and pre-Holocene sequences separated by a basal reflector-R that is interpreted to be as pre-Holocene surface produced by subaerial fluvial erosion of the continental shelves during the lowering period of sea level (e.g. Tesson *et al.,* 1990; Okyar, 1991; Ergin *et al.,* 1992; Park and Yoo, 1998; Salge and Wong, 1988; Okyar and Ediger, 1999; Tezcan and Okyar, 2001).

3.2.1 Acoustic basement (AB)

The acoustic basement (AB) observed on seismic profiles is characterized by chaotic reflection configurations (Appendices 7-21).

The acoustic basement (AB), consisting of the seaward extension of onshore sequences, is generally smooth in relief (Appendices 7-14), except for areas experienced the strong faulting movements (Appendices 15-21). Locally, the acoustic basement shows the outcrop on the sea floor. It occurs in the near shore areas in water depths of less than 20 m (Appendix 14), and in the deep areas where there is no sediment accumulation on the sea floor as a result of the steep slopes (Appendix 20).

Based on the surficial sediment lithology and age of onshore formations, it can be concluded that the composition of the acoustic basement changes with places (Tezcan and Okyar, 2001). It is composed of ophiolite series of Antalya Complex in the western

region, Pliocene-Pleistocene aged clastics of Aksu Basin in the northern region, and metamorphic rock series of Alanya Massif in the eastern regions (Figure 1.11).

3.2.2 Depositional sequence 1

Depositional Sequence 1, overlying the acoustic basement, exhibits the chaotic (Appendices 7-9, 11 and 14) and parallel-subparallel (Appendices 12 and 13) reflections configurations on seismic data. The former reflection configuration indicates coarse and heterogeneous sediments, which accumulated in high-energy environments (Sangree and Widmier, 1977). The latter reflection configuration (parallel-subparallel) implies uniform rates of deposition on a uniformly subsiding shelf or stable basin plain setting (Mithcum *et al.,* 1977b).

The upper boundary of depositional sequence 1 corresponds to an erosional surface that referred to as "reflector R". This erosional surface is delineated by the baselap of the reflectors in the overlying depositional sequences 2 and 3 (Appendices 7-9, 11-14).

Depositional Sequence 1 observed on seismic profile pinches out landward at the depth of the 75 m below the present level. According to sea level curves published for the Eastern Mediterranean regions (e.g. Arbouille and Stanley, 1991), this position of sea level corresponds to approximately 22 000 yrs B.P., (Figure 1.13). This correlation suggests that the depositional sequence 1 accumulated prior to the Holocene transgression.

On the other hand, depositional sequence 1 is entirely absent between the offshore areas of Manavgat and Gazipaşa (Appendices 15-21). This may imply strong erosion with paleocurrents (e.g. Flecker *et al.,* 1998), or alternatively uplift movements (e.g. Woodside, 1977; Özhan, 1998).

3.2.3 Depositional sequence 2

Depositional sequence 2, overlying the depositional sequence 1, shows the chaotic (Appendix 8) and parallel oblique progradational (Appendices 7, 9, 11 and 13) patterns on seismic data. Of these patterns, chaotic configurations are indicative of coarse and heterogeneous sediments accumulated in high-energy environments (Sangree and Widmier, 1977), as outlined before. Parallel oblique prograditional patterns imply depositional conditions with some combination of relatively high sediment supply slow to no basin subsidence, and a still stand sea level to allow rapid basin infill (Mitchum *et al.*, 1977b).

The lower boundary of depositional sequence 2 is delineated by the reflector R (Appendices 7-9, 11 and 13). In particular, depositional sequence 2 off the Acısu and Aksu river mouths (Appendix 1) reflects the appearance of paleo-deltaic deposits with its topset and foreset facies (Appendix 13). The transition from topset and foreset beds is occurred at about 130 m depth. Unfortunately, the bottomset deposit of this paleo-delta is not identified on the seismic data (Appendix 13).

Depositional sequence 2 pinches out landward at the depth of the 110 m below the present sea level. This depth level corresponds to approximately 18 000yrs B.P., (Figure 1.13; Arbouille and Stanley, 1991). Therefore, the sequence 2 is believed to have been deposited during the earlier stages of the Holocene transgression "Flandrian transgession", dated between 22 000 and 18 000 yrs B.P. The same transgressive deposit at the depth of the 110 m was identified on the seismic records collected from the Cilicia Basin (Ediger *et al.*, 1999).

Depositional sequence 2 has not been identified in the seismic profiles collected from the offshore areas of the Selimiye and Gazipaşa (Appendix 1). Here, the absence of depositional sequence 2 appears to be result of strong erosion or alternatively uplift movements.

3.2.3.1 Thickness distribution of depositional sequence 2

The thickness of depositional sequence 2 decreases landward and it disappears in the near shore areas (Appendix 3). In the areas, extending seaward from the coast of Göynük and Hurmaköy, Selimiye and eastern region (Appendix 3), depositional sequences 2 is entirely absent most probably due to erosional and uplift effects on deposition, as explained before.

The maximum thickness value reaching to 40 meters is observed in the south of Güzeloba (Appendix 3). However, some thick accumulations of the depositional sequence 2 ($\geq$ 30 m) also found in the areas of northeast coasts of Cape Çavuş-Kemer, and between off Kumluca and Belekköy coasts (Appendix 3). According to seismic data, these areas exhibit very smooth sub bottom topography.

3.2.4. Depositional sequence 3

Depositional sequence 3, underlying the depositional sequence 4, represents the chaotic (Appendices 7 and 11) and parallel-subparallel (Appendices 8-10, 12-14) reflection configurations similar to that of depositional sequence 1. Within this sequence some occurrences of the fill seismic facies units are existed (Appendices 7, 9-11). These types of seismic facies are commonly interpreted as the result of topographic irregularities, which occur in response to erosion that are later filled or covered by the transgressive sediments (Brown and Fisher, 1979).

The upper boundary of depositional sequence 3 (bottom of depositional sequence 4) is characterized by topographic irregularities (Appendices 7-14). These irregularities are probably formed by erosional and/or tectonic activities prevailing in the area.

Depositional sequence 3 pinches out landward at the depth of the 50 m, which corresponds to approximately 11 500 yrs B.P., (Figure 1.13; Arbouille and Stanley, 1991). Therefore, it can be concluded that the depositional sequence 3 is formed

between 18 000 and 11 500 yrs B.P. The existence of same type deposit, dated between 18 000 and 11500 yrs B.P., is reported from the Cilicia Basin (Ediger *et al.*, 1999) and the offshore Göksu delta (Okyar and Ediger, 1998).

Depositional sequence 3 is not observed on the seismic profiles collected from the submarine canyon off Hurmaköy and the offshore areas of the Selimiye and Gazipaşa (Appendix 1) most probably due to erosion and uplift processes.

3.2.4.1 Thickness distribution of depositional sequence 3

In general, the thickness of depositional sequence 3 begins to reduce towards the shore until disappear (Appendix 4). Additionally, this sequence is absent in the submarine canyon area of Hurmaköy, off the Selimiye coast and in the eastern region (Appendix 4), probably caused by erosion and uplift.

The maximum thickness value, reaching to 50 m is seen southeast of Göynük (Appendix 4). Some areas in the northern region (i.e. in offshore area extending between the Kumluca and Selimiye) exhibit low thickness values (Appendix 4). In these areas, thickness of depositional sequence 3 is less than 10 m in thick (Appendix 4). Here, the isopach contours show small closures, which resemble minor depressions. These features are consistent with the fill seismic facies units that interpret from high-resolution seismic data (Appendices 7, 9-11 and 14).

3.2.5 Depositional sequence 4

Depositional sequence 4 is characterized by sigmoid progradational (Appendix 7) and parallel (Appendices 8-21) reflection configurations. As outlined before, parallel reflections patterns are indicative of the uniform rates of deposition on a uniformly subsiding shelf or stable basin plain setting (Mitchum *et al.*, 1977b). Sigmoid progradational patterns indicate relatively low sediment supply, relatively rapid basin

subsidence and/or rapid rise in sea level (Mitchum *et al.,* 1977b). A relatively low energy regime is interpreted (Brown and Fisher, 1979).

In general, the depositional sequence 4 covering the pre-deposited sequence (1-3) and the acoustic basement (AB) forms a sedimentary wedge towards the open sea (Appendices 7-20). The top of this sequence forms the present sea floor. The internal layering of the depositional sequence 4 is concordant with the surface (Appendices 7-21).

Occurrences of fill seismic facies within depositional sequence 4 are also observed on seismic profiles (Appendices 14, 16 and 17). In particular, the depositional sequence 4 in near shore waters off Kemer-Hurmaköy (Appendix 1) exhibits the seaward progradation of the coast, presumably in the form of fan-delta progradation (Appendices 8 and 10). These features appear to be result of excessive sediment transport from the coastal areas (e.g. Okyar, 1991; Ergin *et al.,* 1992).

The depositional sequence 4 is being deposited during the last 11 500 yrs B.P., (e.g. Arbouille and Stanley, 1991). It covers the whole sea floor area of the Antalya Bay. On the other hand, this sequence has been subjected to strong faulting, especially offshore areas between the Selimiye and Gazipaşa (Appendices 15-21).

3.2.5.1 Thickness distribution of depositional sequence 4

In general, the thickness of depositional sequence 4 increases towards the shore (Appendix 5) in contrast to pre-deposited sequences 2 and 3. As explained in sub-bottom stratigraphy section, this sequence forms a sedimentary wedge towards the open sea.

Thickness of depositional sequence 4 tends to increase in near shore areas. These areas are generally characterized by the small embayment and the river inputs. The maximum sedimentation of this sequence occurs in the fan-delta progradation areas. In these areas; the southwest of Göksu River and the south of Güzeloba, depositional sequence is more

than 40 m in thickness (Appendix 5). Seaward, the thickness of depositional sequence 4 begins to decrease and reduces to zero (Appendix 5). The absence of sequence 4 in the deep areas is probably due to steep gradient of the slopes.

3.2.6 Total sediment thickness distribution of the Holocene sequences

Except for the submarine canyon area off Hurmaköy, the thickness value of Holocene sequences varies from 5 to 80 meters in the western region (Appendix 6).

The areas from south to north are; northeast of the Cape Çavuş, east of the Kesme River mouth, northeast of the Kemer and southeast of the Hurmaköy (Appendix 6), characterized by thick sediment accumulations (≥55 m). The maximum thickness value, which is measured to be as 80 meters, occurs at about 5 km southeast of the Düden River mouth (Appendix 6).

In the northern region, the thickness of Holocene sequences ranges between 5 and 50 meters (Appendix 6). In general, the thickness values tend to reduce in near-shore areas (Appendix 6). The maximum thickness value, reaching to 50 meters, is observed at about 12 km southwest of Belekköy (Appendix 6).

In contrast to western and northern regions, the eastern region is characterized by low thickness values (Appendix 6). Here, the thickness of Holocene sequences varies from 2 to 15 meters (Appendix 6). The maximum thickness value of Holocene sequences, reaching to 20 meter, is observed between off the Niprit and Karpuz River mouths (Appendix 6).

All these findings indicate that the thickness of the Holocene sequences are controlled by sea level changes, basin subsidence and erosional/depositional conditions. Of these, sea level changes and basin subsidence are believed to have been played important roles in the deposition of Holocene sequences in the past.

Under present conditions, it seems that gently sloping shelf areas are site of sediment accumulation, whereas deepest areas (i.e. submarine canyon of Hurmaköy and narrow shelf off eastern region) are mostly eroded.

CHAPTER FOUR
CONCLUSIONS

This research is the first detailed investigation carried out in the continental shelf of Antalya Bay. Therefore, bathymetric and seismic data pertinent to the aims of the study will assist the future research activities in the area. Additionally, results in this study are important for two main reasons; scientific interest and offshore engineering surveys. It is believed that this kind of study will contribute to scientific investigations relating to the Quaternary Geology of Turkey. In view of the offshore engineering, informations on the sea floor topography and sub bottom nature of the sea floor in the Antalya Bay will be useful for offshore site surveys (foundation studies for offshore platforms, harbor development, and cable/pipeline crossing surveys).

Bathymetric map of the Antalya Bay suggests that the continental shelf in the bay varies greatly in width and character. In general, shelf areas having the gentle slopes of $< 2°$ occur in the western and northern regions that receive greater sediments from the rivers on land. The shelf is very steep ($>2°$) or absent in the eastern region.

Submarine canyons that extend across the shelf to the basin slope incise some areas of the sea floor in the Antalya Bay. These submarine canyons have been formed by sedimentary and/or tectonic processes. Topographic irregularities observed on echo-sounding data indicate the slumping, faulting and bottom current actives on the sea floor in the Antalya Bay. Therefore, the present configuration of the bathymetry is basically controlled by sedimentation and tectonics of the Antalya Bay. Smaller scale bathymetric features are, however, mainly controlled by slumping, faulting and current processes.

The interpretation of seismic data has revealed the existence four distinct depositonal sequences above the acoustic basement in the study area.

The acoustic basement consists of the seaward extension of the onshore sequences. Its composition corresponds to ophiolite series of Antalya Complex in the western region, Pliocene-Pleistocene aged clastics of Aksu Basin in the northern region, and metamorphic rock series of Alanya Massif in the eastern region. Although its upper surface seems to be smooth, it exhibits irregular topography in some areas, which subjected to faulting movements. In the areas of steep slopes and of non-deposition, acoustic basement is exposed on the sea floor.

Depositional sequence 1 observed on seismic data is the oldest seismostratigraphic unit of the surveyed area. It pinches out at the depth of 75 m on the acoustic basement. According to the sea level curve, sea level reached to this position at about 22 000 yrs B.P. Therefore, it is concluded that the depositon of this sequence was occurred before the Holocene transgression. The absence of this sequence in most parts of the surveyed areas is related to strong erosion and/or to uplift movements.

In the surveyed area, the depositional sequence 2 pinches out at the depth of 110 m on the reflector-R. The available sea-level curve implies that sea level reached to this position at about 18 000 yrs B.P. From this, it can be concluded that depositional sequence 2 was deposited during the earlier stages of Holocene transgression between 22 000 and18 000 yrs B.P. Off the Acısu and Aksu River mouths this sequence was developed in the shape of palaeo-delta. In some parts of the surveyed area, this sequence is absent, probably caused by the erosion and/or the uplift movements. The maximum thickness of depositional sequence 2 was measured as 40 meters in the northern region.

The depositional sequence 3 pinches out at the depth of 50 m on the reflector-R. According to the published sea level curve, this level corresponds to 11 500 yrs B.P. Therefore, this unit is interpreted to have been deposited during the period from about 18 000 yrs B.P. until 11 500 yrs B.P. Occurrences of fill seismic facies within this depositonal sequence indicates the erosional structures that are later filled by sediments. Lack of the depositional sequence 3 in some areas is probably due to erosion and/or the

uplift movements. The maximum thickness value of the depositional sequence 3, reaching to 50 m, occurs in the eastern region.

The depositional sequence 4 observed on seismic data is the youngest seismostratigraphic unit of the surveyed area. Its upper boundary forms the present sea floor. This sequence has been deposited during the last 11 500 years. The thickness of the depositional sequence 4 decreases and forms a sedimentary wedge towards the sea. In front of the fan-delta type of progradational areas it becomes thicker ($\geq$40 meters).

The basal reflector-R in the seismic profiles represents an erosional unconformity cutting the stratified structures of the underlying acoustic basement (AB) and the depositional sequence 1. It forms the lower boundary of the overlying youngest depositional sequence 4, especially in near shore areas. In addition, the depositional sequences (2 and 3) pinch out on the reflector R. Such seismic boundary relationships and erosional unconformities imply pre-Holocene erosional surfaces produced by the subaerial fluvial erosion of the continental shelves.

REFERENCES

Akay E., Uysal S., Poisson A., Cravette J., and Müller C., 1985. Stratigraphy of the Antalya Neogene Basin, Bull. Geol. Soc. Turkey, 28, 105-119.

Aksu A.E., Calon T., Piper D.W.J., Turgut S. and Izdar E., 1992. Architecture of later orogenic Quaternary basins in northeastern Mediterranean Sea. Tectonophysics, 210, 191-213.

Arbouille D. and Stanley D.J., 1991. Late Quaternary evolution of the Burullus lagoon region, north-central Nile delta, Egypt. Mar.Geol., 99, 45-66.

Badley M.E., 1985. Practical Seismic Interpretation. Prentice-hall, Englewood Cliffs, NJ, 266 pp.

Blumenthal M., 1947. Geologie der Taurusketten im hinterland von Seydişehir und Beyşehir: Maden Tetkik Arama Enst., Bull., 67, 105-109, Ankara.

Blumenthal M., 1951. Recherche geologiques dans le Taurus occidental dans l'arriere-pays d'Alanya. Maden Tetkik Arama Enst., Publ., ser. D, 5, 134pp, Ankara.

Boggs S.Jr., 1987. Principle of Sedimentology and Stratigraphy. Macmillan, New York, 784 pp.

Bowen D.Q., 1978. Quaternary Geology, A stratigraphic Framework for Multidisciplinary Work. Pergamon Press Ltd., Headington Hill Hall, Oxford England, 221pp.

Bremer H., 1971. Geology of the Coastal Regions of Southwestern Turkey, in A.S. Campell (editor), Geology and History of Turkey, Petr.Expl.Soc.Libya.

Brown JR. LF. and Fisher W.L., 1977. Seismic Stratigraphic Interpretation of Depositional Systems: Examples from Brazilian Rift and Pull-Apart Basins. In: C.E. Payton (editor), Seismic Stratigrapy – Applications to hydrocarbon Exploration, Memoir: 26, Am. Assoc. Petrol. Geol., Tulsa, Oklahoma, 213-248.

Brown JR. LF. and Fisher W.L., 1980. Seismic Stratigraphic Interpretation and Petroleum Exploration. AAPG Continuing Education Course Note Series 16, Am. Assoc. Petrol. Geol., Tulsa, Oklahoma, 125pp.

Brunn J.H, 1974. Le probleme de l'origin des nappes et de leur translations dans les Taurids occidentals. Bull. Soc. geol. France, 16, 101-106.

Brunn J.H, Dumont J.F., De Graciansky P.C., Gutnic M., Juteau T., Marceaux J., Monod O. and Poisson A., 1971. Outline of the geology of the western Taurides. In: A.S. Campell (editor), Geology and History of Turkey, Pet. Explor. Soc. Libya, Tripoli, 225-255.

Burger D., 1990. The travertine complex of Antalya Southwest Turkey. Zeitschrift für Geomorphologie. Neue Forschung, Suppl. Bd., 77, 25-46.

Canals M., Catafau E. and Serra J., 1988. Sedimentary structure and seismic facies of the inner continental shelf north of the the Ebro Delta (northwestern Mediterranean Sea). Cont. Shelf Res., 8, 961-977.

Curray J.R., 1961. Late Quaternary Sea Level: A Discussion. Geol. Soc. Am. Bull., 72, 1707-1712.

Curray J.R, 1964. Transgressions and Regressions. In: R.L. Miller (editor), Papers in Marine Geology, Shepard Commemorative Volume, The Macmillan Company, New York, 175-203.

Damuth J.E., 1980. Use of high frequency (3.5-12kHz) echograms in the study of near bottom sedimentation processes in the deep sea: a review. Mar. Geol., 38, 51-75.

Delaune-Mayere M., Marcoux C., Parrot J.F. and Poisson A., 1977. Modele d'evolution Mesozoique de la paleomarge Tethysienne au niveau des nappes radiolaritiques et ophiolitiques du Taurus Lycien, d'Antalya et du Baer-Bassit. In: Biju-Duval B. and Montadert L. (editors), Structural history of the Mediterranean basins, Technip, Paris, 79-94.

DSİ (2000), Devlet Su İşleri Genel Müdürlüğü (unpublished data), Ankara.

Ediger V., 1987. Recent sedimentation in the Bay of Anamur. M.S. Thesis, Institute of Marine Sciences, Erdemli, İçel, Turkey, 127pp.

Ediger V., Okyar M. and Ergin M., 1993. Seismic stratigraphy of the fault controlled submarine canyon/valley system on the shelf and upper slope of Anamur Bay, Northeastern Mediterranean Sea. Mar. Geol., 115, 129-142.

Ediger V., Okyar M., Tekiroğlu S.E., Görür N. and Çağatay N., 1999. Kilikya-Adana Havzası Kıta Sahanlığının Geç Kuvaterner Çökellerinin Araştırılması-I Projesi Sonuç Raporu.TÜBİTAK Ulusal Deniz Jeolojisi ve Jeofiziği Araştırma Programı, Proje Kod No: YDABÇAG-599/G, 69pp.

EİE (1995), Aylık Ortalama Akımlar, Hidrolik Etütler Dairesi Başkanlığı,Ankara.

Emiliani C. And Filint R.F., 1980. The Pleistocene record. In: M.N. Hill (general editor), The sea, ideas and observations on progress in the study of the seas, the earth beneath the sea history, 3, Robert E.Kriger Publishing Company Huntington, New York, 888-927.

Ergin M., Okyar M., Timur K., 1992. Seismic stratigraphy and late Quaternary sediments in inner and mid-shelf areas of eastern Mersin Bay, Northeastern Mediterranean Sea. Marine Geology 104, 73-91.

Erinç S., 1963. Yeryüzünün Şekillenmesi. İ. Ketin (editor), Umumi Jeoloji II. Kısım, Arzkabuğunun Dış Olayları ve Yeryüzü Şekilleri. İst. Teknik Üniversitesi Kütüphanesi Sayı: 513, Berksoy matbaası, İstanbul, Türkiye, 1-13.

Evans G., 1970. The recent sedimentation of Turkey and the adjacent Mediterranean and Black Seas: A review. In: A.S. Campell (editor), Geology and History of Turkey, Pet. Explor. Soc. Libya, Tripoli, 385-406.

Fairbanks R.G., 1989. A 17 000-year glacio-eustatic sea level record: influence of glacial melting rates on the Younger Dryas event and deep ocean circulation. Nature, 342, 637-642

Flecker R., Robertson A.H.F., Poisson A. and Müller C., 1995. Facies and tectonic significance of two contrasting Miocene Basins in south coastal Turkey. Terra Res., 7, 221-232.

Flecker R., Ellam R.M., Müller C., Poisson A., Robertson A.H.F., Turner J., 1998. Application of Sr isotope stratigraphy and sedimentary analysis to the origin and evolution of the Neogene basins in the Isparta Angle, southern Turkey. Tectonophysics, 298, 83-101.

Glover C., 1996. Plio-Quaternary Sediments and Neotectonics of the Isparta Angle, southwest Turkey. Ph.D. thesis. Univ. Edinburgh.

Glover C. and Robertson A.H.F., 1993. Delta progradation and terrace formation related to regional uplift, Aksu Basin, Southern Turkey. 7th Eur. Union Geosci. Strasburg, Terra Abstract(1) of Terra Nova, 5, 279.

Glover C. and Robertson A.H.F., 1998a. Neotectonic intersection of the Aegean and Cyprus tectonic arcs: extensional and strike-slip faulting in the Isparta Angle, SW Turkey. Tectonophysics, 298, 103-132.

Glover C. and Robertson A.H.F., 1998b. Role of regional extension and uplift in the Plio-Pleistocene evolution of Aksu Basin, SW Turkey. J. Geol. Soc. London, 155, 365-387.

Got H., Bouye C. and Mirabile L., 1987. Lithoseismic analyse: a method for sedimentology. Oceanol. Acta, 10, 1-13 (in French with English Abstr.).

Hayward A.B., 1984. Miocene clastic sedimentation related to the emplacement of the Lycian Nappes and the Antalya Complex, SW Turkey. In: J.F.Dixon and A.H.F. Robertson, The Geological Evolution of the Eastern Mediterranean, Geological Society Special Publication,17, 287-300.

Hecht A., Pinardi N., Robinson A., 1988. Currents, water masses, eddies and jets in the Mediterranean Levantine Basin. Journal of Physical Oceanography, 18, 1320-1353.

Herman Y., 1972. Quaternary Eastern Mediterranean Sediments: Micropaleontology and Climatic Record. In: D.J. Stanley (editor), The Mediterranean Sea: A Natural Sedimentation laboratory. Dowden Hutchinson and Ross, Inc. Stroudsburg, Pennsylvania, 129-147.

Kennet J.P., 1982. Marine Geology. Prentice-Hall, Inc., Englewood Cliffs, New Jersey, 813pp.

King C.A.M., 1972. Beaches and Coasts. Edward Arnold Publishers Ltd, London. 570pp.

Klaus A. and Ledbetter M.T., 1988. Deep-sea sedimentary processes in the Argentina Basin revealed by high-resolution seismic records (3.5kHz echograms). Deep-Sea Res., 35/6, 899-917.

Komar P.D., 1976. Beach Processes And Sedimentation. Prentice-Hall Inc., Englewood Cliffs, New Jersey, 429pp.

Macdonald D.I.M., 1991. Sedimentation, Tectonics and Eustasy. Sea-level Changes at Active Margins. Spec. Publ. Int. Assoc. Sedimentol., 12, 518 pp.

Malanotte-Rizzoli P., Manca B.B, Ribera d'Alcala M., Theocharis A., Brenner S., Budillon G., Özsoy E., 1999. The Eastern Mediterranean in the 80s and in the 90s: the big transition in the intermediate and deep circulation. Dyn. Atmos. Oceans, 29, 365-395.

Malovitsky Ya.B., Emelyanov E.M., Kazakov O.V., Moscalenko V.N., Osipov G.V., Shimkus K.M. and Chumakov I.S., 1975. Geological structure of the Mediterranean sea floor (based on geological and geophysical data). Mar. Geol., 18(4), 231-261.

Milliman J.D. and Emery, 1968. Sea levels during the Past 35 000 years. Science 62, 1121-1123.

Mitchum JR. R.M., Vail P.R. and Thompson III S., 1977a. Seismic Stratigraphy and Global Changes of Sea Level Part 2: The Depositional Sequences as a Basic Unit for Stratigraphic Analysis. In: C.E Payton (editor), Seismic Stratigrapy – Applications to hydrocarbon Exploration, Memoir: 26, Am. Assoc. Petrol. Geol., Tulsa, Oklahoma, 53-82.

Mitchum JR. R.M., Vail P.R. and Sangree J.B., 1977b. Seismic Stratigraphy and Global Changes of Sea Level Part 6: Stratigraphic Interpretation of Seismic Reflections Patterns in Depositional Sequences. In: C.E Payton (editor), Seismic Stratigrapy – Applications to hydrocarbon Exploration, Memoir: 26, Am. Assoc. Petrol. Geol., Tulsa, Oklahoma, 117-133.

Monod O., 1976. La courbure d Isparta une mosaique de blocs autochtones surmontes de nappes composites a la junction de l'arc hellenique et de l arc taurique. Bull. Soc. geol. France, 18, 521-532.

Morner N.A., 1971. Eustatic changes during the lat 20 000 years and a method of separating the isostatic and eustatic factors in an uplifted area. Palaeogeography, Paleoclimatology, Paleoecology, 9, 153-181.

Okay A.I. and Özgül N., 1984. HP/LT metamorphism and the structure of the Alanya Massif, Southern Turkey: an allochthonous composite tectonic sheet. In: J.F.Dixon and A.H.F. Robertson (editors), The Geological Evolution of the Eastern Mediterranean, Geological Society Special Publication, 17, 429-439.

Okyar M., 1991. The late Quaternary transgression and its associated submarine stratigraphy of Mersin Bay between the Göksu and the Seyhan delta: a geophysical approach. Ph.D. Thesis, Institute of Marine Sciences, Erdemli, İçel, Turkey, 156pp.

Okyar M. and Ediger V., 1997. Sea-floor sediments and bedforms around Turkey, revealed by side scan sonar imagery. Oceanologica Acta, 20(5), 673-685.

Okyar M. and Ediger V., 1998. Göksu Delta'sının Kuvaterner Jeolojisinin Sismik Yöntemlerle İncelenmesi Alt Projesi Sonuç Raporu. TÜBİTAK Ulusal deniz Jeolojisi ve Jeofiziği Araştırma Programı, Proje Kod No: YDABÇAG-374/G, 89pp.

Okyar M. and Ediger V., 1999. Seismic evidence of shallow gas in the sediment on the shelf off Trabzon, southeastern Black Sea. Cont. Shelf Res., 19, 575-587.

Özhan G., 1988. Sismik yansıma verileri ışığında Kuzeydoğu Akdeniz. Geol. Bul. of Turkey, 31, 51-62.

Özsoy E., Oğuz T., Latif M.A. and Ünlüata Ü., 1987. Kuzey Levant Denizinin Oşinografisi, Fiziksel Oşinografi cilt, 1. Ulusal Deniz Ölçme ve İzleme Programı, Akdeniz Alt Projesi. METU-Institute of Marine Sciences, Erdemli, İçel/Turkey, 183pp.

Özsoy E., Hecht A., Ünlüata Ü., 1989. Circulation and hydrography of the Levantine Basin. Results of POEM coordinated experiments 1985-1986. Prog. Oceanog., 22, 125-170.

Özsoy E., Hecht A., Ünlüata Ü., Brenner S., Sur H.I., Bishop J., Latif M.A., Rozentraub Z., Oğuz T., 1993. A synthesis of the Levantine Basin circulation and hydrography, 1985-1990. Deep Sea Res., II, 40(6): 1075-1119.

Park S.C. and Yoo D.G., 1988. Depositional history of Quaternary sediments on the continental shelf off the southeastern coast of Korea (Korea Strait). Mar. Geol. 79, 65-75.

Poisson A., 1984. The extentions of the Ionian trough into southwestern Turkey. In: J.F.Dixon and A.H.F. Robertson, The Geological Evolution of the Eastern Mediterranean, geological Society Special Publication,17, 241-250.

Pentecost A., 1995. The Quaternary travertine deposits of Europe and Asia Minor. Quaternary Sciences Reviews, 14, 1005-1028.

Reuber I., 1984. Mylonitic ductile shear zones within tectonites and cumulates as evidence for an oceanic transform fault in the Antalya ophiolite, SW Turkey. In: J.F.Dixon and A.H.F. Robertson, The Geological Evolution of the Eastern Mediterranean, Geological Society Special Publication,17, 319-334.

Ricou L.E., Argyriadis I. and Lefevre R., 1974. Proposition d'une origin interne pour les nappes d 'Antalya et le massif d'Alanya (Taurus occidentals, Turquie). Bull. Soc. geol. France, 16, 107-111.

Ricou L.E., Argyriadis I. and Marcoux J., 1975. L'axe calcaire du Taurus, un alignemant de fenetres arabo-africains sous des nappes radiolaritiques, ophiolitiques et metamorphiques. Bull. Soc. geol. France, 17, 1024-1044.

Robertson A.H.F. and Woodcock N.H., 1981. Bilelyeri Group, Antalya Complex, S.W. Turkey: deposition on a Mesozoic passive continental margin. Sedimentology, 28, 381-399.

Robertson A.H.F. and Dixon J.E., 1984. Introduction: aspects of the geological evolution of the Eastern Mediterranean. In: J.F.Dixon and A.H.F. Robertson, The Geological Evolution of the Eastern Mediterranean, Geological Society Special Publication,17, 1-74.

Robertson A.H.F. and Woodcock N.H., 1984. The SW segment of the Antalya Complex, Rturkey as a Mesozoic- Tertiary Tethyan continental margin. In: J.F.Dixon and A.H.F. Robertson, The Geological Evolution of the Eastern Mediterranean, Geological Society Special Publication,17, 251-271.

Robertson A.H.F., 1993. Mesozoic-Tertiary sedimentary and tectonic evolution of Neotethyan carbonate platforms, margins and small ocean basins in the Antalya Complex, Southwest Turkey. In: Frostick L.E. and Steel R. (editors), Tectonic Controls and Signatures in Sedimentary Successions. Spec. Publ. Int. assoc. Sedimentol., 20, 415-465.

Robertson A.H.F., 1998. Mesozoic-Tertiary tectonic evolution of the easternmost Mediterranean area: Integration of marine and land evidence. In: A.H.F. Robertson, K.-C. Emeis, C. Richter and A. Camerlenghi (editors), Proceeding of the Ocean Drilling Program, Scientific Results, 160, 723-782.

Roos D.A., Uchubi E. and Bowin C.O., 1974. Shallow structure of Black Sea. In: E.T. Degens and D.A. Roos (editors), The Black Sea-Geology, Chemistry and Biology. AAPG Mem., 20, 11-34.

Salge U. and Wong H.K., 1988. Seismic stratigraphy and Quaternary sedimentation in the Skagerrak (northeastern North Sea). Mar. Geol., 81, 159-174.

Sangree J.B. and Widmier J.M., 1977. Seismic Stratigraphy and Global Changes of Sea Level Part 9: Seismic Interpretation of Clastic Depositional Facies. In: C.E Payton (editor), Seismic Stratigrapy – Applications to hydrocarbon Exploration, Memoir: 26, Am. Assoc. Petrol. Geol., Tulsa, Oklahoma, 213-248.

Sangree J.B. and Widmier J.M., 1979. Interpretation of depositional facies from seismic data. Geophysics, 44, 131-160.

Shepard F.P., 1973. Submarine Geology. Harper & Row, Publishers, New York, 517pp.

Stefanon A., 1985. Marine Sedimentology Through Modern Acoustical Methods: II. Uniboom. Boll. Ocenol. Teor. Appl., 3, 113-144.

Şengör A.M.C., Yılmaz Y. and Sungurlu O., 1984. Tectonics of the Mediterranean Cimmerides: nature and evolution of the western termination of Paleo-Tethys. In: J.F.Dixon and A.H.F. Robertson, The Geological Evolution of the Eastern Mediterranean, Geological Society Special Publication,17, 77-112.

Taviani M. and Rossi S., 1989. Salt-related deformations in the deep Antalya Basin: preliminary results of the Mac Gan Cruise. Mar. Geol., 87, 5-13.

Tezcan D. and Okyar M., 2001. Antalya Körfezi batı kıta sahanlığının geç Kuvaterner sedimanlarının sismik stratigrafisi. Türkiye Kuvaterneri Çalıştayı, Bildiri Özetleri Kitapçığı, 21-22 Mayıs. İTÜ Avrasya Yer Bilimleri Enstitüsü, Süleyman Demirel Kültür Merkezi, İTÜ, İstanbul, 45.

Tesson M., Gensous B., Allen G.P. and Ravenne Ch., 1990. Late Quaternary deltaic lowstand wedges on the Rhone continental shelf, France. Mar. Geol., 91, 325-332.

Theoharis A., Gergopoulos D., Lascaratos A., Nittis K., 1993. Water masses circulation in the central region of the Eastern Mediterranean (E: Ionian, S. Aegean and NW Levantine). Deep Sea Res., II, 40, 6: 1121-1142.

Turkish Navy Chart, 1970. Alanya – Anamur Burnu Map, 1/100 000 scale, sheet 324.

Turkish Navy Chart, 1974. Antalya Körfezi Map, 1/100 000 scale, sheet 322.

Turkish Navy Chart, 1975. Kaş – Anamur Burnu Map, 1/300 000 scale, sheet 32.

Turkish Navy Chart, 1976. İleri Burnu – Alanya Map, 1/100 000 scale, sheet 323.

TÜBİTAK Project (199Y074). Antalya Körfezi Kıta Sahanlığının Geç Kuvaterner Jeolojisi: Sedimantolojik, Mineralojik, Jeokimyasal ve Sismik Araştırmalar. Yer Deniz ve Atmosfer Bilimleri ve Çevre Araştırma Grubu, TÜBİTAK, Ankara, (in prep.).

Ünlüata Ü., 1986. A Review of the Physical Oceanography of the Levantine and the Aegean Basins of the Eastern Mediterranean in Relation to Monitoring and Control of Pollution, Institute of Marine Sciences, METU Technical Report, 55pp.

Vail P.R., Mitchum JR. R.M. and Thompson III S., 1977. Seismic Stratigraphy and Global Changes of Sea Level Part 3: Relative changes of sea level from coastal onlap. In: C.E Payton (editor), Seismic Stratigrapy – Applications to hydrocarbon Exploration, Memoir: 26, Am. Assoc. Petrol. Geol., Tulsa, Oklahoma, 53-82.

Waldron J.W.F., 1984. Structural history of the Antalya Complex in the Isparta Angle, Southwest Turkey. In: J.F.Dixon and A.H.F. Robertson, The Geological Evolution of the Eastern Mediterranean, geological Society Special Publication,17, 273-286..

Woodside J.M., 1977. Tectonic elements and crust of the eastern Mediterranean Sea. Mar. Geophy. Res., 3, 317-354.

Yılmaz P.O., 1984. Fossil and K-Ar data for the age of the Antalya Complex, SW Turkey. In: J.F.Dixon and A.H.F. Robertson, The Geological Evolution of the Eastern Mediterranean, Geological Society Special Publication,17, 335-348.

APPENDICES

APPENDIX 1: Location map of the survey lines in Antalya Bay. The echo-sounding profiles (Figures 3.1-3.6) and high-resolution seismic profiles (Appendices 7-21) presented in this study are given in solid lines.

APPENDIX 2: Bathymetric map of the Antalya Bay. Contour intervals are: 10 m from the coast to 20 m depth, and 20 m between the depths of 20 and 220 m.

APPENDIX 3: Isopach map showing the thickness of depositional sequence 2 in Antalya Bay. Contours in meters. Note, dash lines indicate seaward limit of the studied area.

APPENDIX 4: Isopach map showing the thickness of depositional sequence 3 in Antalya Bay. Contours in meters. Note, dash lines indicate seaward limit of the studied area.

APPENDIX 5: Isopach map showing the thickness of depositional sequence 4 in Antalya Bay. Contours in meters. Note, dash lines indicate seaward limit of the studied area.

APPENDIX 6: Isopach map showing the total sediment thickness of the Holocene sequences (2, 3 and 4) above the reflector-R in Antalya Bay. Contours in meters. Note, dash lines indicate seaward limit of the studied area.

APPENDIX 7: High-resolution seismic profile (for location see Appendix 1) from the western region showing depositional sequences (1, 2, 3 and 4) and acoustic basement (AB). Note the reflector-R marks the pre-Holocene erosional surface. a and b : two fill seismic facies units in depositional sequence 3.

APPENDIX 18

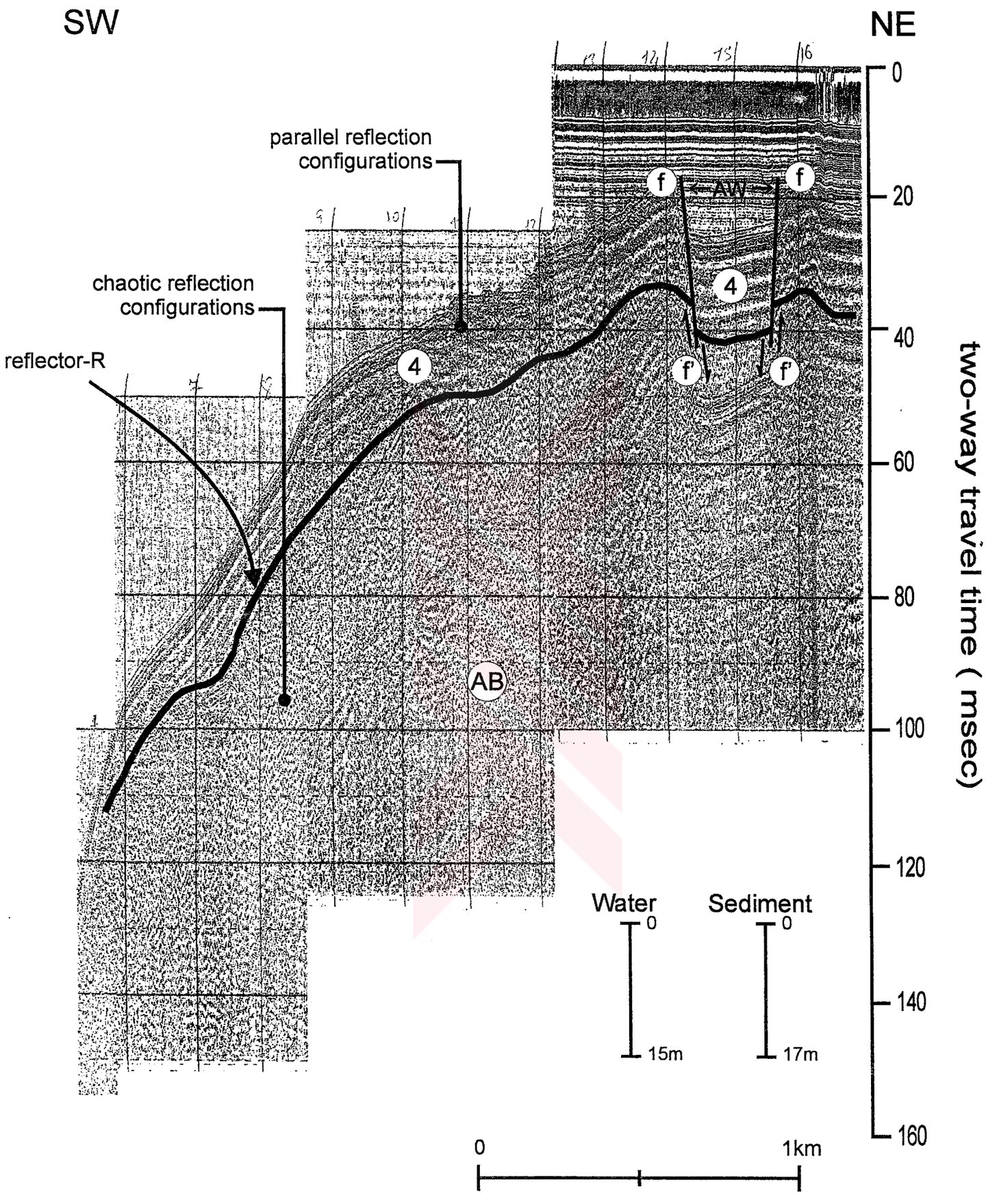
SW
NE
parallel reflection configurations
chaotic reflection configurations
reflector-R
f
AW
f
f'
f'
4
4
AB
0
20
40
60
80
100
120
140
160
two-way travel time (msec)
Water
0
15m
Sediment
0
17m
0
1km

APPENDIX 17

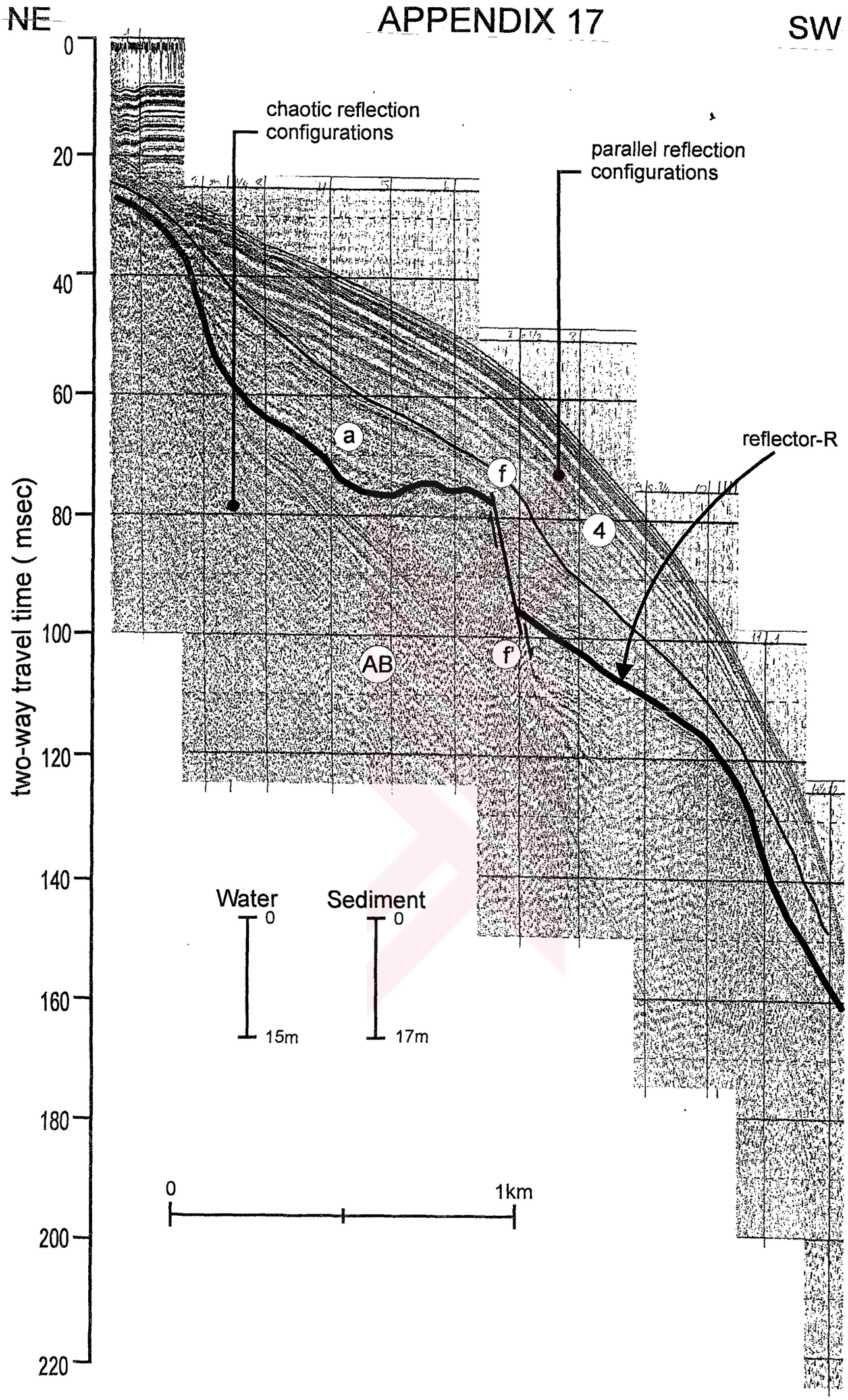
NE
SW
chaotic reflection configurations
parallel reflection configurations
reflector-R
a
f
f'
4
AB
two-way travel time (msec)
0
20
40
60
80
100
120
140
160
180
200
220
Water
Sediment
0
0
15m
17m
0
1km

APPENDIX 16

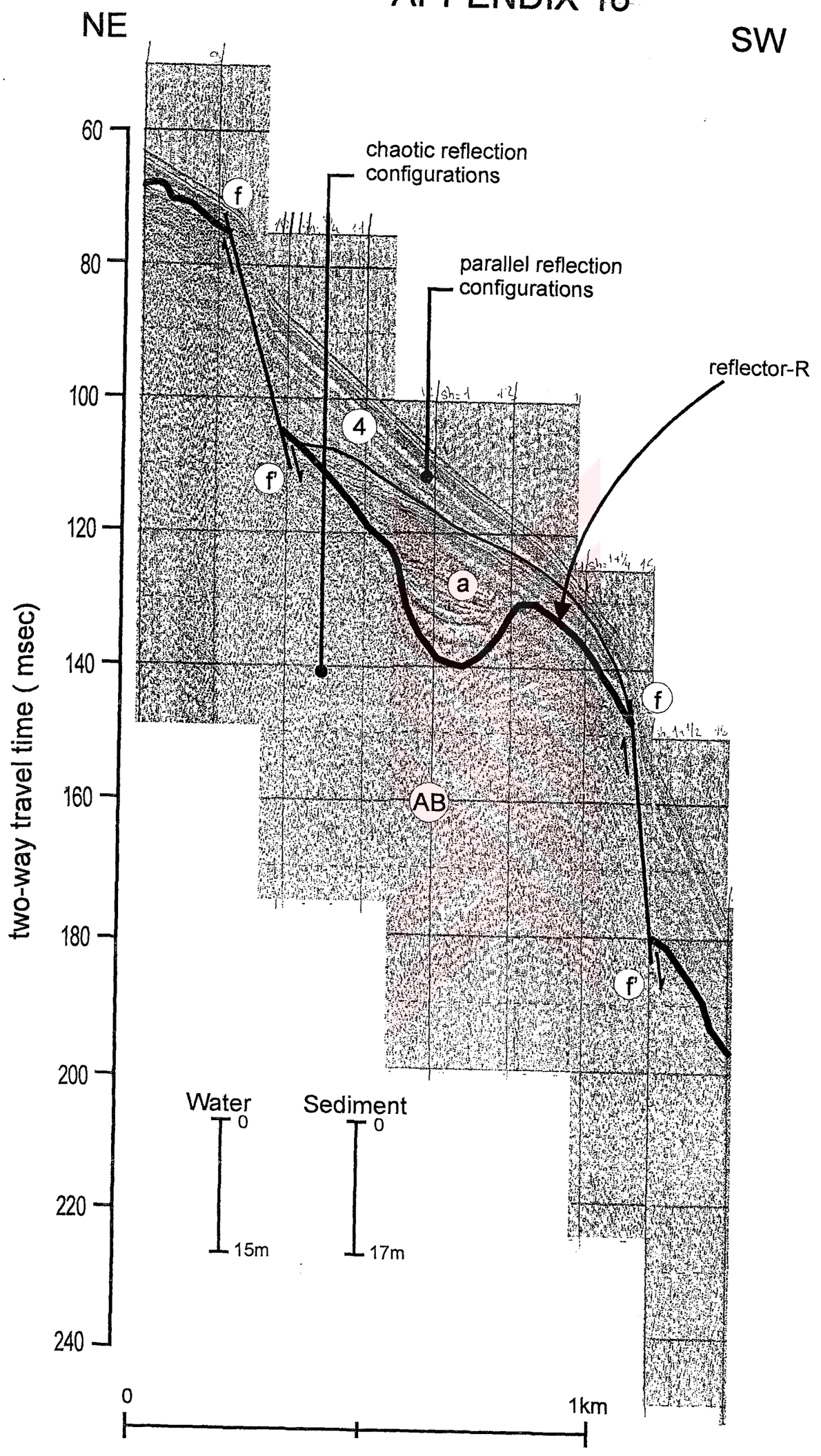
NE
SW
60
80
100
120
140
160
180
200
220
240
two-way travel time (msec)
chaotic reflection configurations
parallel reflection configurations
reflector-R
f
f'
4
a
AB
f
f'
Water
0
15m
Sediment
0
17m
0
1km

APPENDIX 15

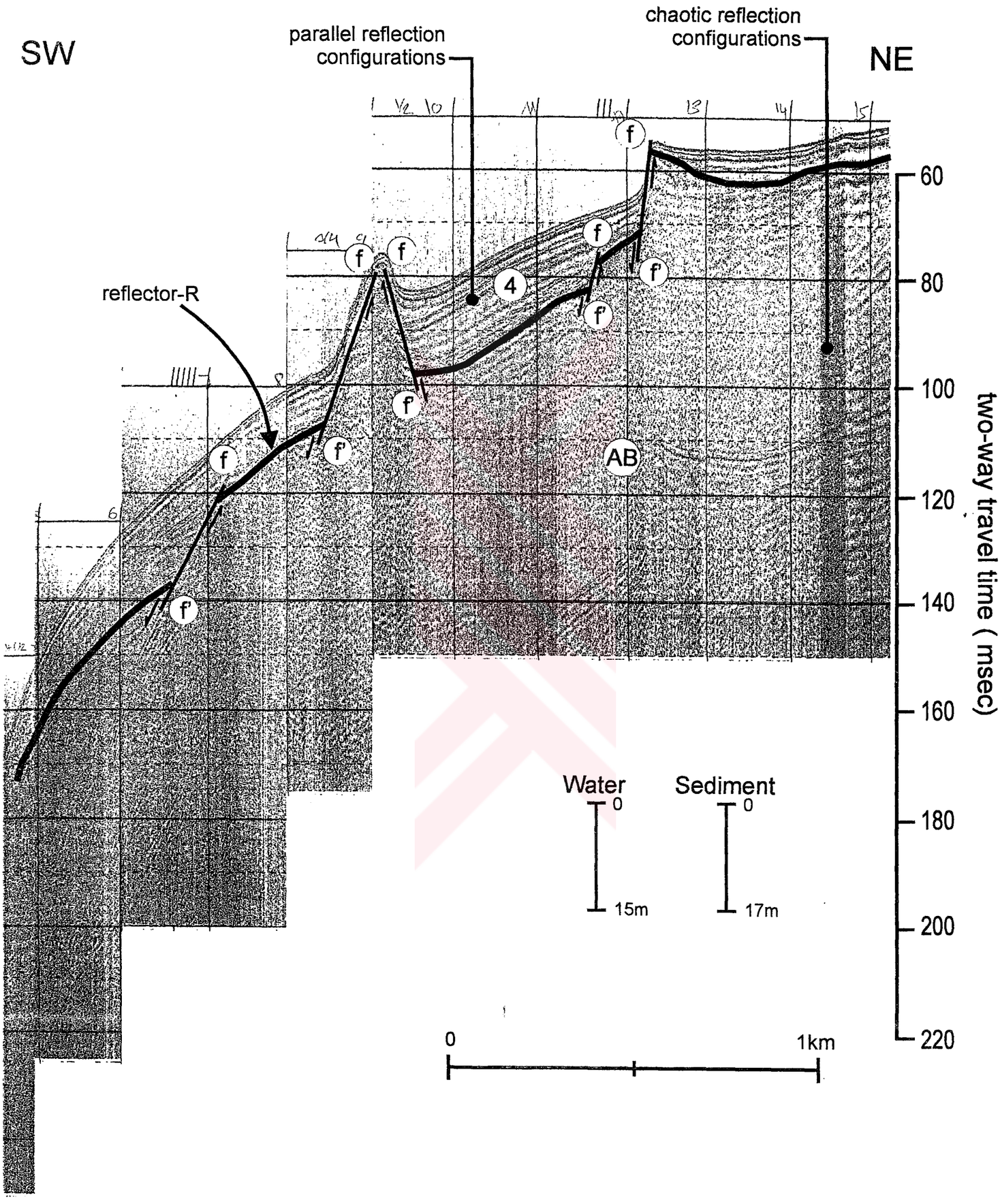
SW
NE
parallel reflection configurations
chaotic reflection configurations
reflector-R
f
f'
4
AB
60
80
100
120
140
160
180
200
220
two-way travel time (msec)
Water
0
15m
Sediment
0
17m
0
1km

APPENDIX 14

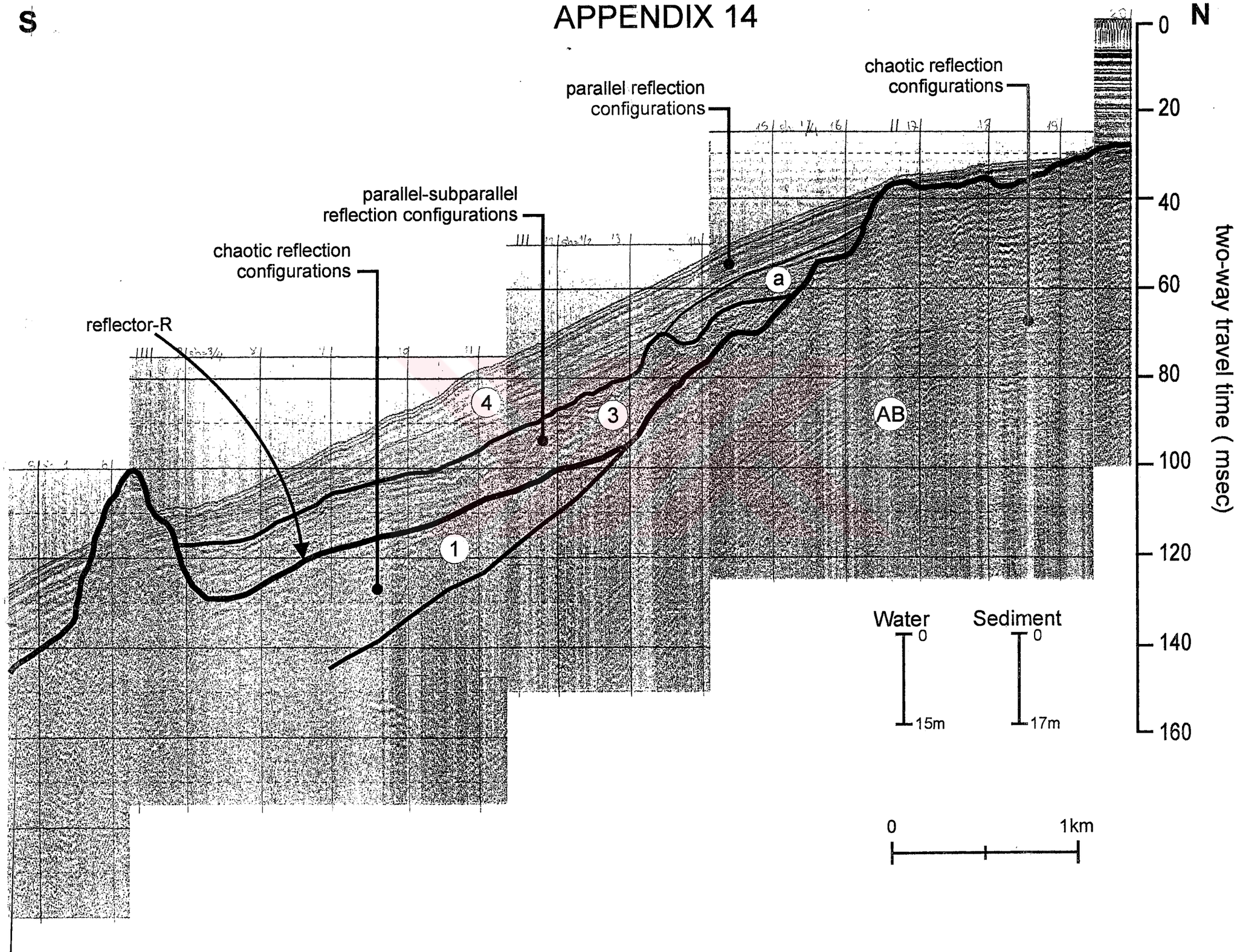
S
N
parallel reflection configurations
chaotic reflection configurations
parallel-subparallel reflection configurations
chaotic reflection configurations
reflector-R
a
4
3
AB
1
0
20
40
60
80
100
120
140
160
two-way travel time (msec)
Water
Sediment
0
15m
0
17m
0
1km

APPENDIX 13

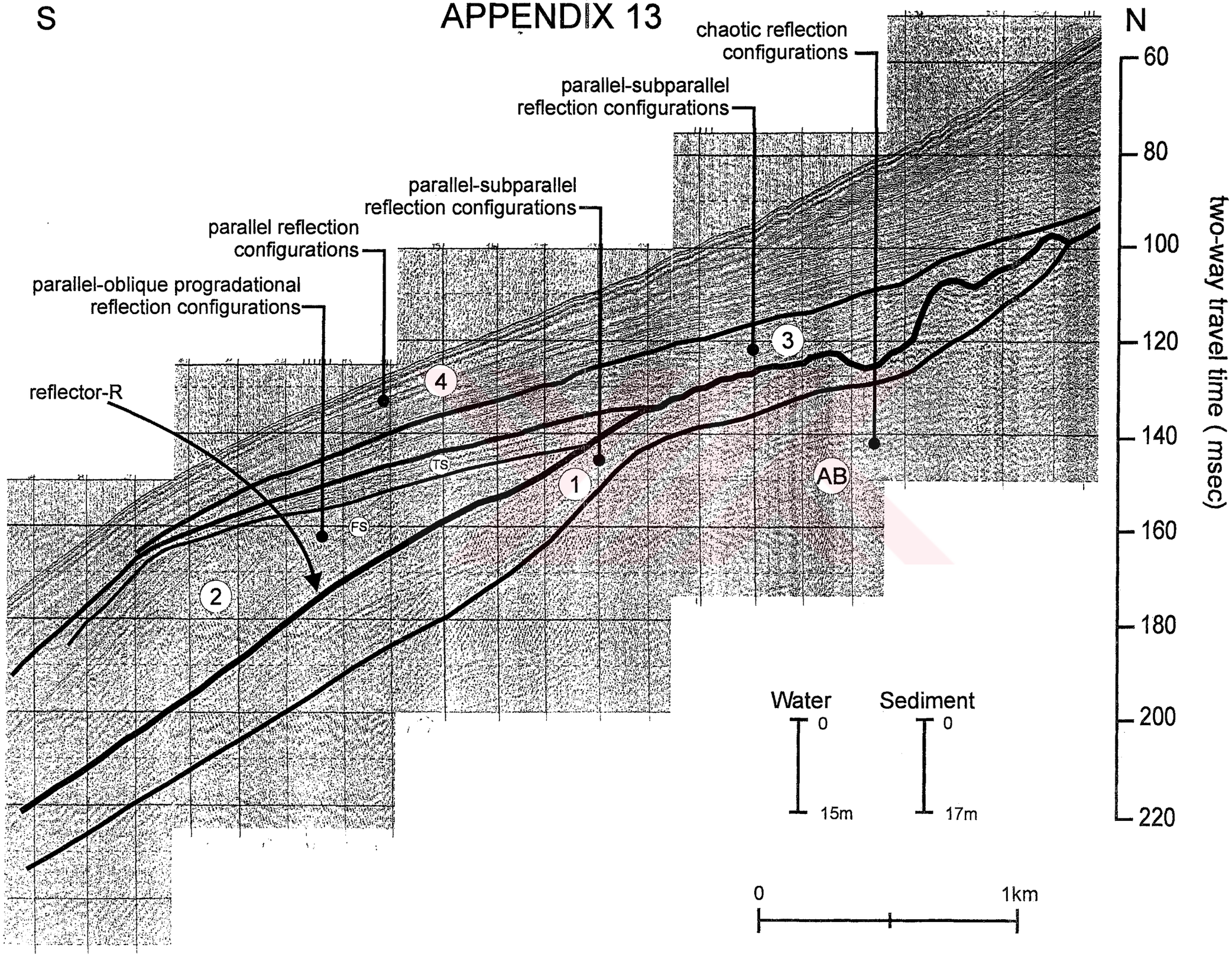
S
N
chaotic reflection configurations
parallel-subparallel reflection configurations
parallel-subparallel reflection configurations
parallel reflection configurations
parallel-oblique progradational reflection configurations
reflector-R
TS
FS
AB
1
2
3
4
60
80
100
120
140
160
180
200
220
two-way travel time (msec)
Water
0
15m
Sediment
0
17m
0
1km

APPENDIX 12

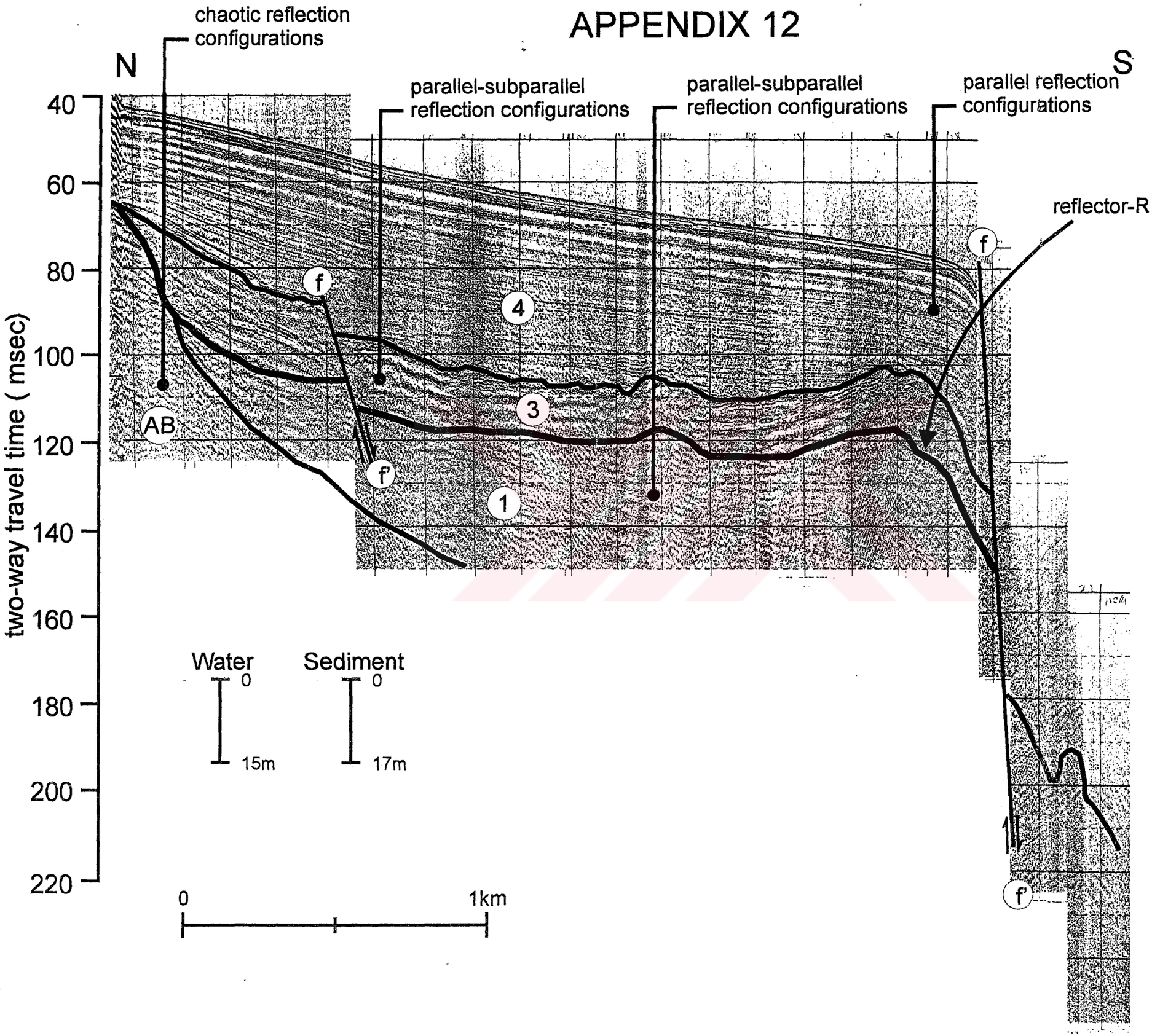
chaotic reflection configurations
N
S
parallel-subparallel reflection configurations
parallel-subparallel reflection configurations
parallel reflection configurations
reflector-R
40
60
80
100
120
140
160
180
200
220
two-way travel time (msec)
f
f'
AB
4
3
1
Water
0
15m
Sediment
0
17m
0
1km

APPENDIX 11

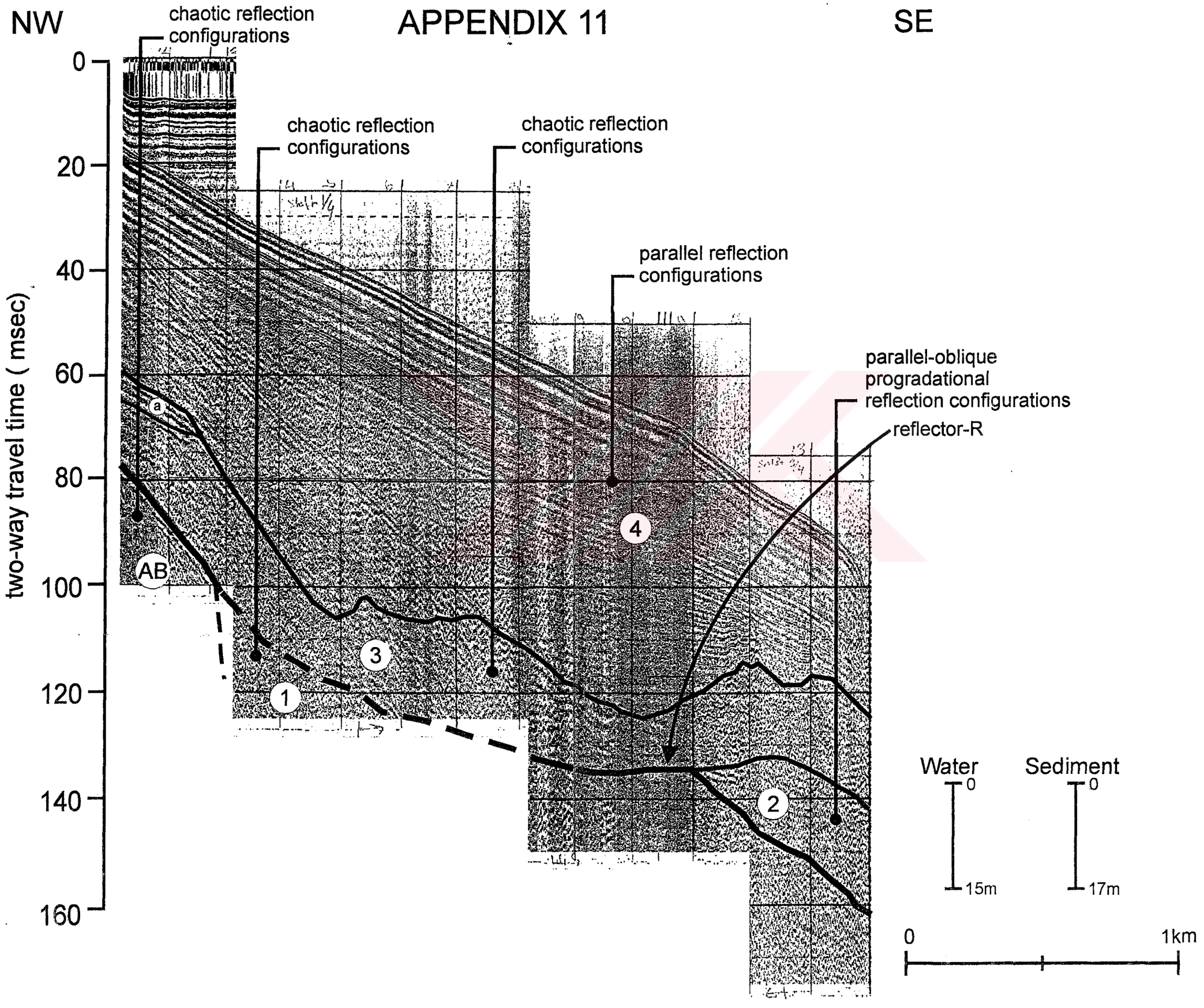
NW
SE
chaotic reflection configurations
chaotic reflection configurations
chaotic reflection configurations
parallel reflection configurations
parallel-oblique progradational reflection configurations
reflector-R
two-way travel time (msec)
0
20
40
60
80
100
120
140
160
a
AB
1
2
3
4
Water
0
15m
Sediment
0
17m
0
1km

APPENDIX 10

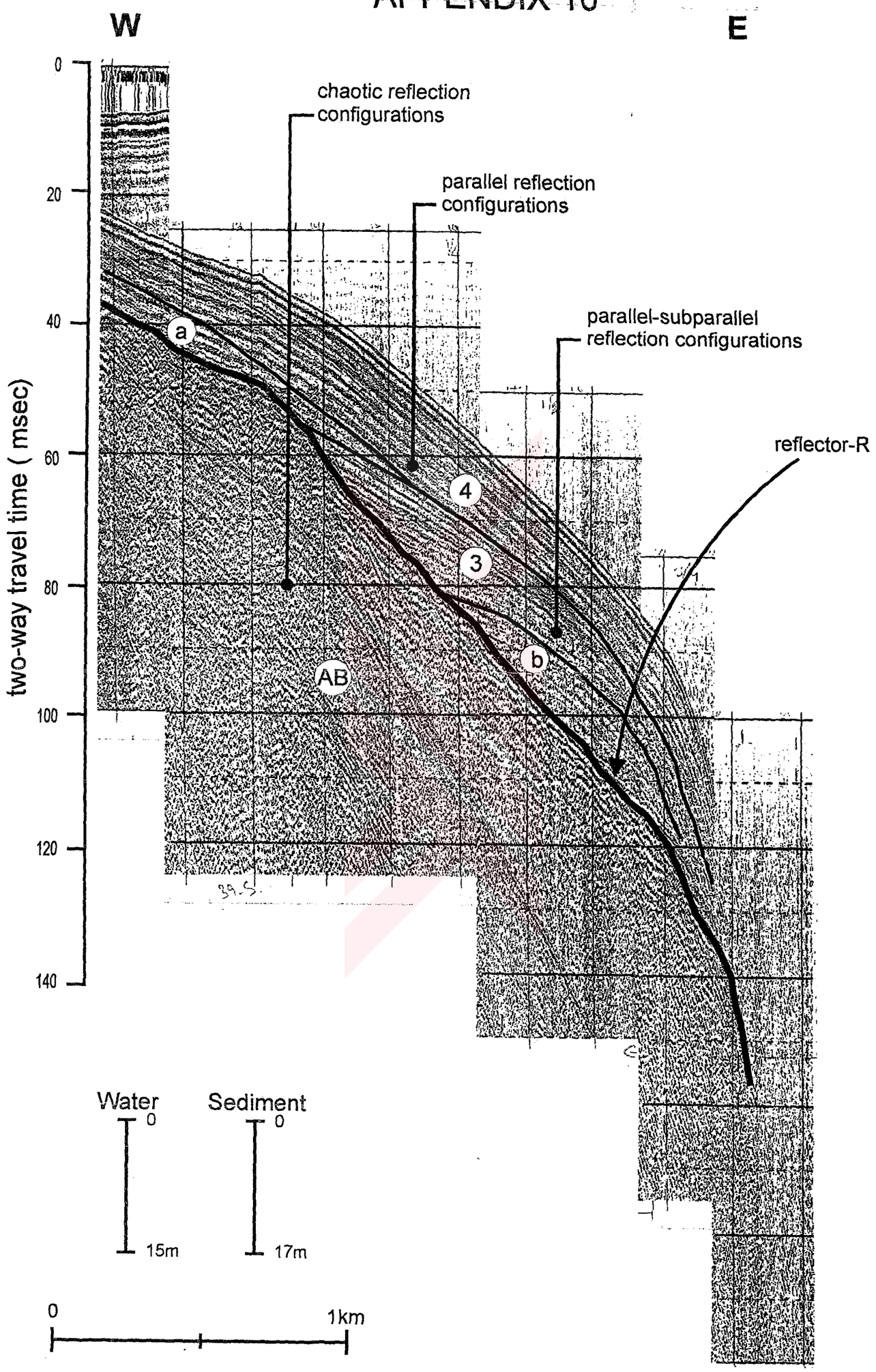
W
E
0
20
40
60
80
100
120
140
two-way travel time (msec)
chaotic reflection configurations
parallel reflection configurations
parallel-subparallel reflection configurations
reflector-R
a
4
3
b
AB
39.5
Water
0
15m
Sediment
0
17m
0
1km

APPENDIX 9

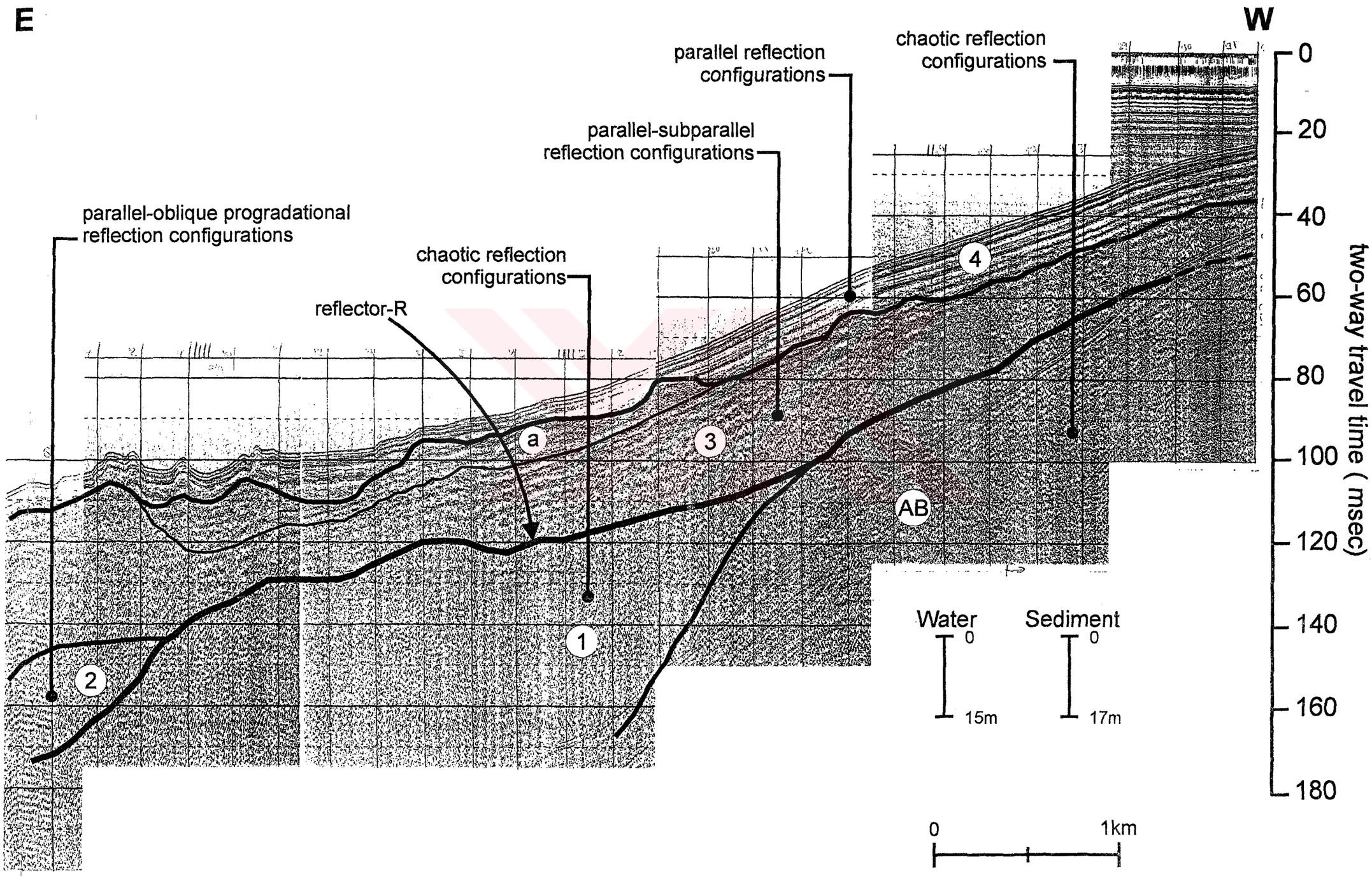
E
W
parallel reflection configurations
chaotic reflection configurations
parallel-subparallel reflection configurations
parallel-oblique progradational reflection configurations
chaotic reflection configurations
reflector-R
4
a
3
AB
1
2
Water
0
15m
Sediment
0
17m
0
1km
0
20
40
60
80
100
120
140
160
180
two-way travel time (msec)

APPENDIX 8

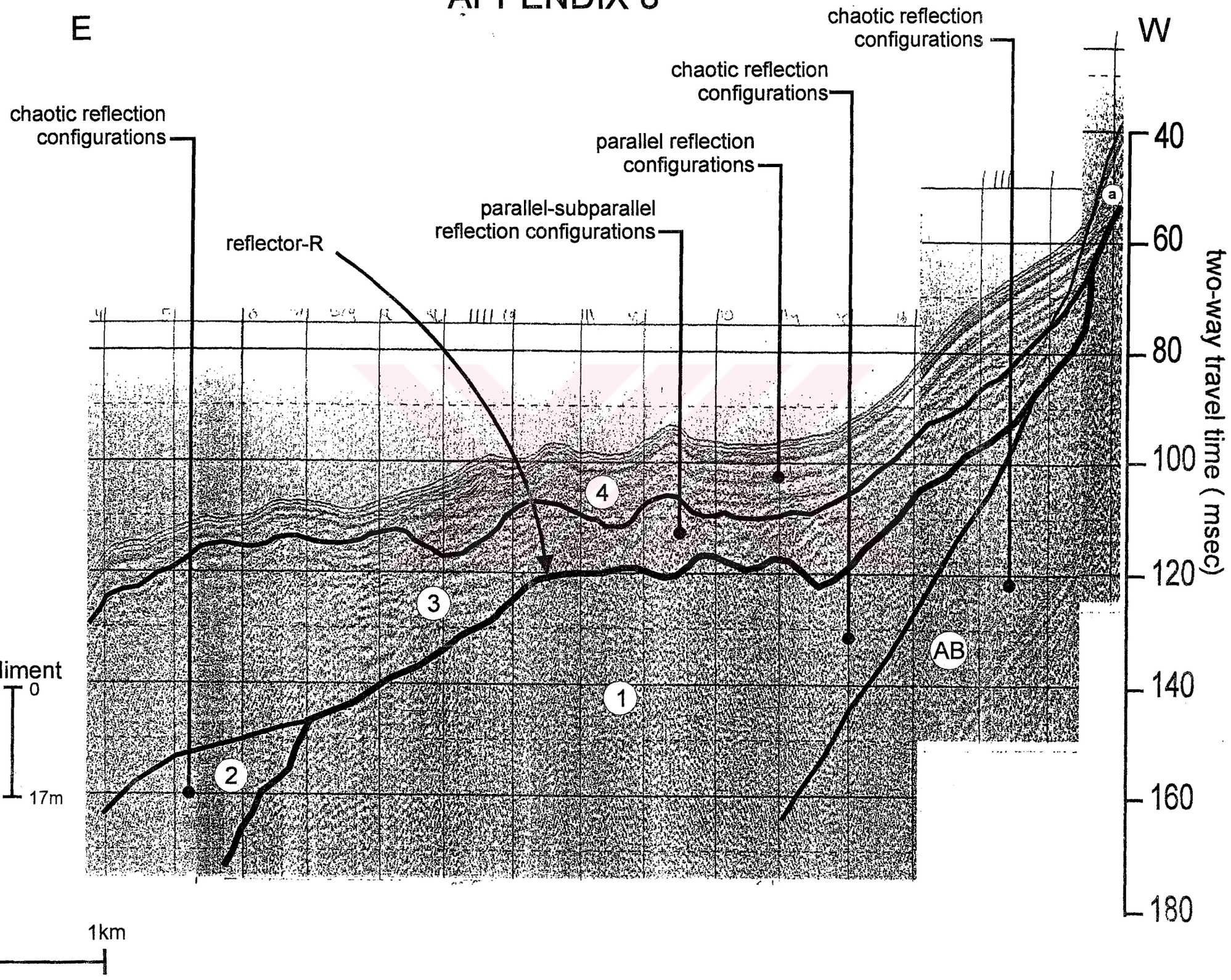
E
W
chaotic reflection configurations
chaotic reflection configurations
chaotic reflection configurations
parallel reflection configurations
parallel-subparallel reflection configurations
reflector-R
a
4
3
2
1
AB
two-way travel time (msec)
40
60
80
100
120
140
160
180
Water
0
15m
Sediment
0
17m
0
1km

APPENDIX 7

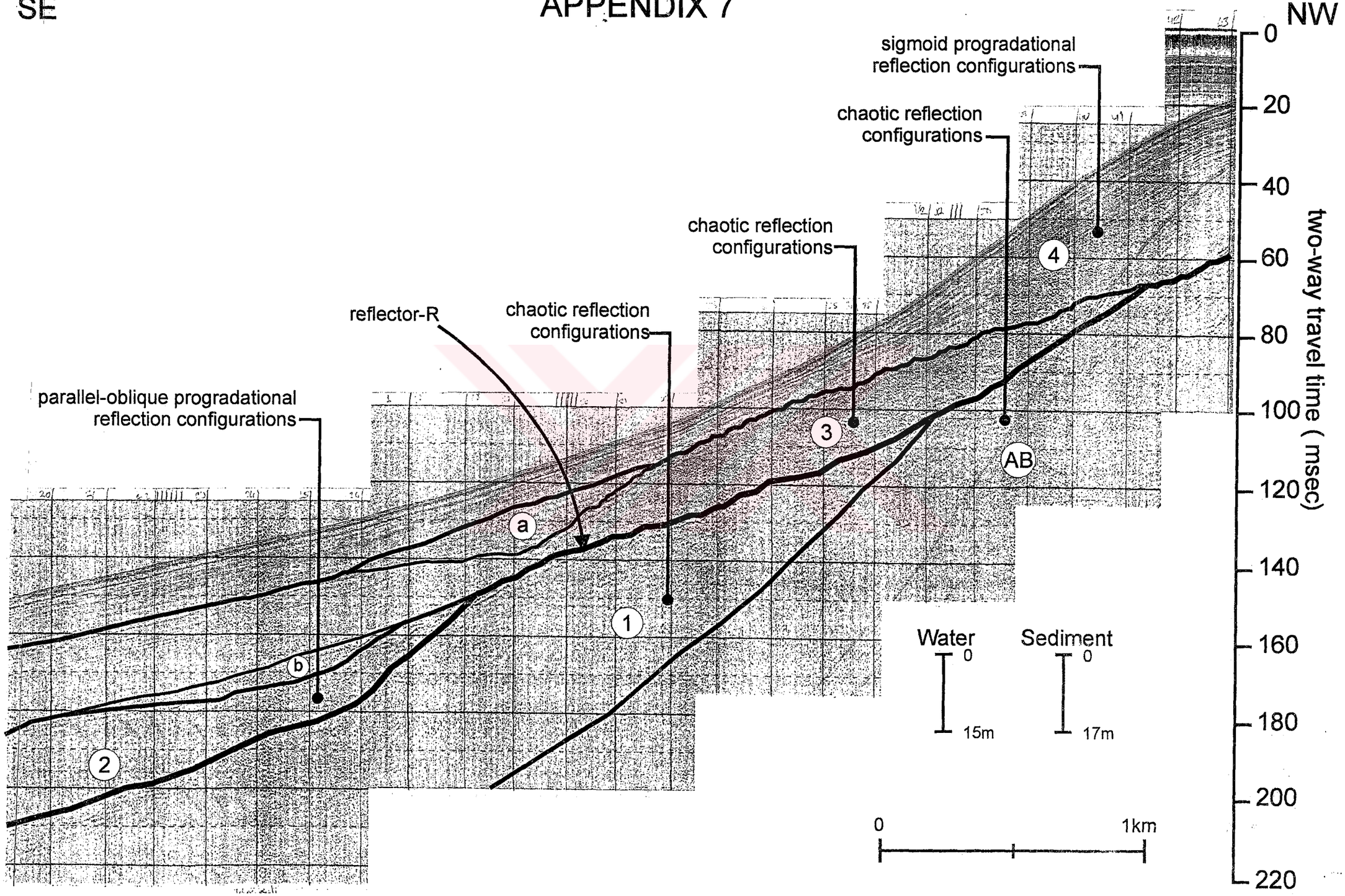
SE
NW
sigmoid progradational reflection configurations
chaotic reflection configurations
chaotic reflection configurations
reflector-R
chaotic reflection configurations
parallel-oblique progradational reflection configurations
4
3
AB
a
b
1
2
Water
0
15m
Sediment
0
17m
0
1km
0
20
40
60
80
100
120
140
160
180
200
220
two-way travel time (msec)

APPENDIX 6

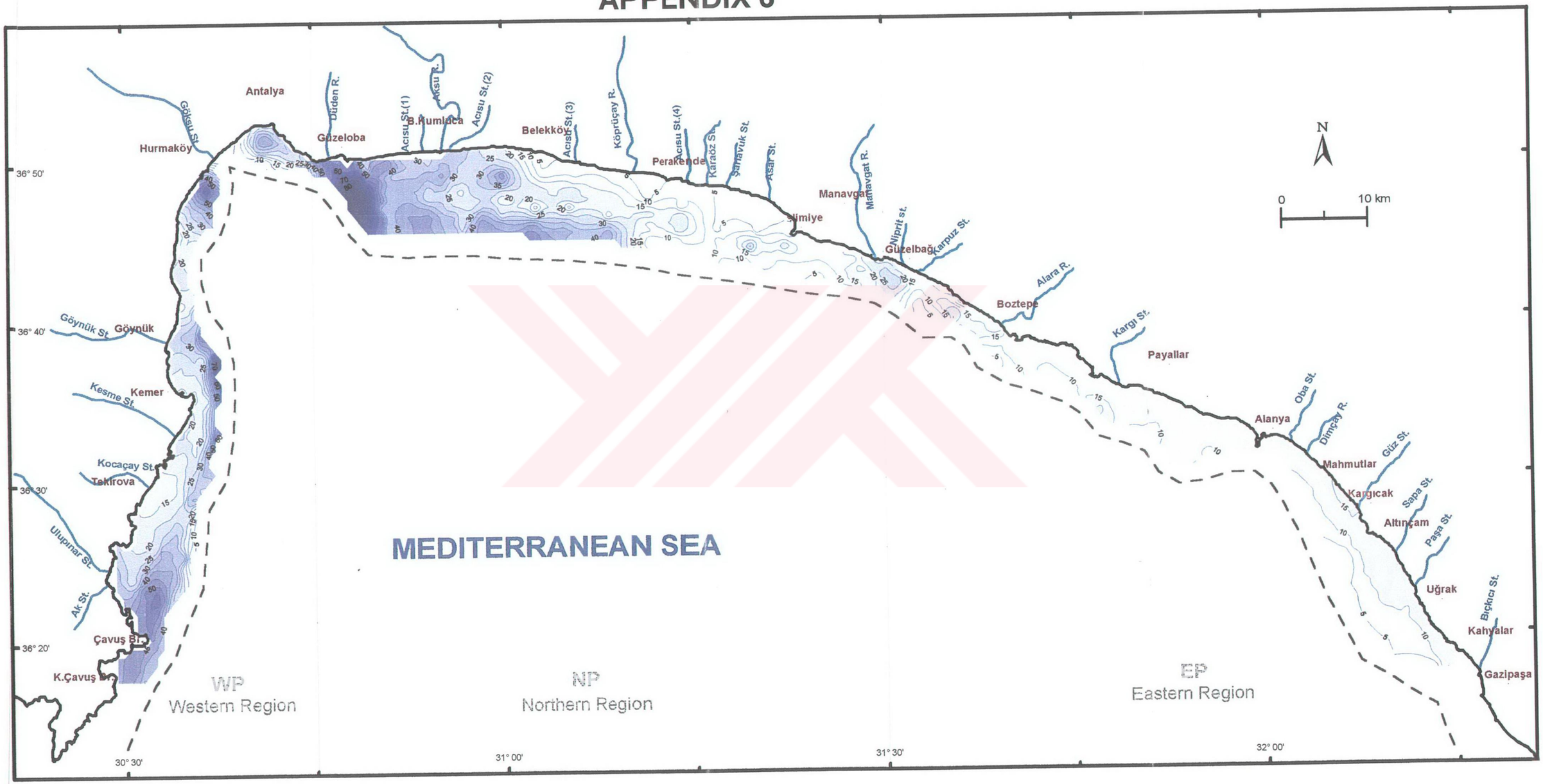
Antalya
Göksu St.
Hurmaköy
Düden R.
Güzeloba
Acısu St.(1)
B.Kumlaca
Aksu R.
Acısu St.(2)
Belekköy
Acısu St.(3)
Köprüçay R.
Perakende
Acısu St.(4)
Karaöz St.
Sanavvuk St.
Asar St.
Manavgat
Manavgat R.
Nİprit st.
Güzelbağ
Karpuz St.
Alara R.
Boztepe
Kargı St.
Payallar
Oba St.
Alanya
Dimçay R.
Güz St.
Mahmutlar
Kargıcak
Sapa St.
Altınçam
Paşa St.
Uğrak
Bıçkıcı St.
Kahyalar
Gazipaşa
Göynük St.
Göynük
Kesme St.
Kemer
Kocaçay St.
Tekirova
Ulupınar St.
Ak St.
Çavuş Br.
K.Çavuş Br.
36° 50'
36° 40'
36° 30'
36° 20'
30° 30'
31° 00'
31° 30'
32° 00'
N
0
10 km
MEDITERRANEAN SEA
WP
Western Region
NP
Northern Region
EP
Eastern Region

APPENDIX 5

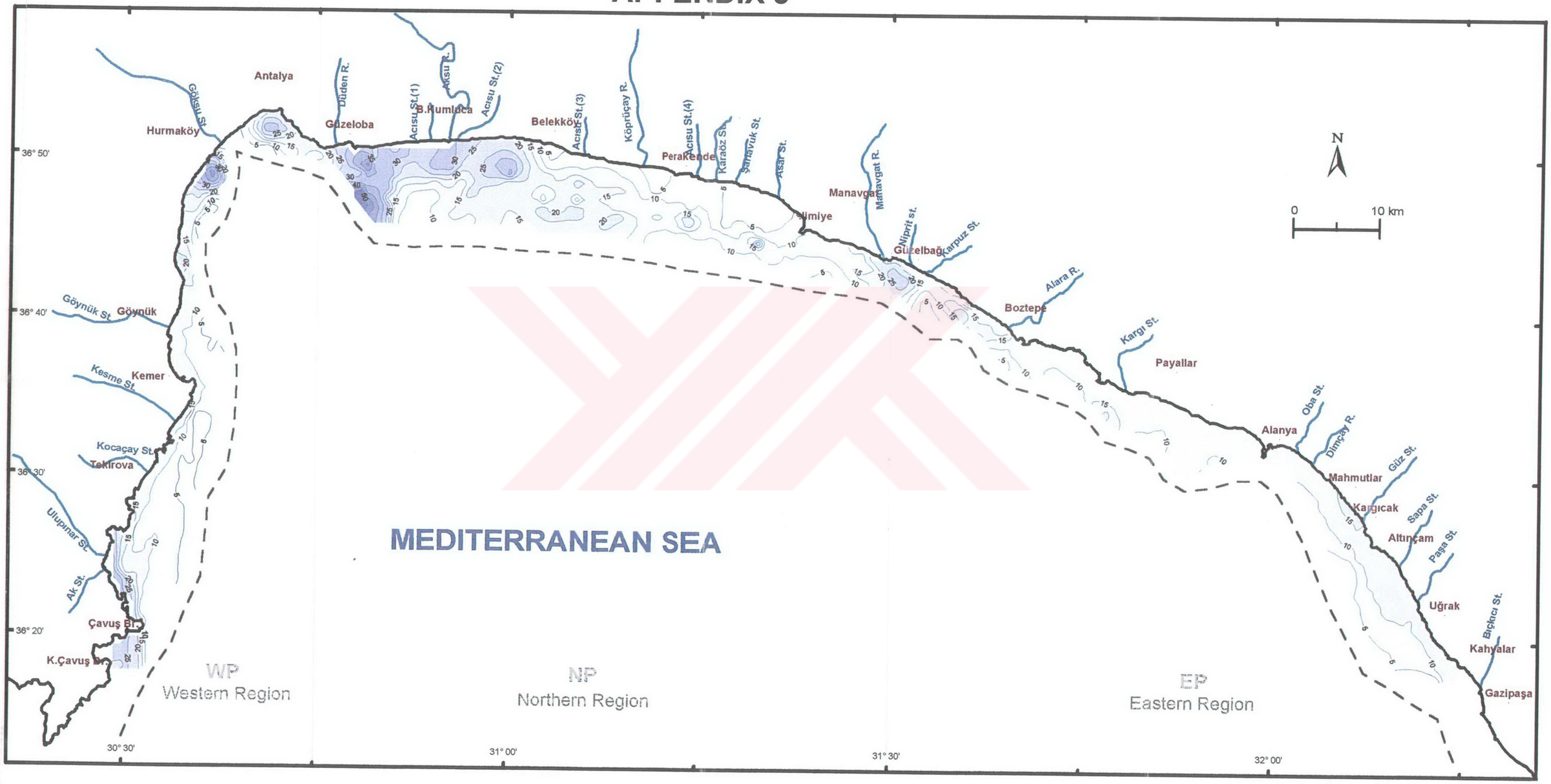
Antalya
Hurmaköy
Gölsu St.
Düden R.
Güzeloba
Acısu St.(1)
B.Kumluca
Acısu R.
Acısu St.(2)
Belekköy
Acısu St.(3)
Köprüçay R.
Acısu St.(4)
Perakende
Karaöz St.
Şahnavuk St.
Asar St.
Manavgat
Manavgat R.
limiye
Nilüfer st.
Güzelbağ
Karpuz St.
Alara R.
Boztepe
Kargı St.
Payallar
Oba St.
Alanya
Dimçay R.
Güz St.
Mahmutlar
Kargıcak
Sapa St.
Altınçam
Paşa St.
Uğrak
Bıçkıcı St.
Kahyalar
Gazipaşa
Göynük St.
Göynük
Kemer
Kesme St.
Kocaçay St.
Tekirova
Ulupınar St.
Ak St.
Çavuş Br.
K.Çavuş Br.
36° 50'
36° 40'
36° 30'
36° 20'
30° 30'
31° 00'
31° 30'
32° 00'
N
0
10 km
MEDITERRANEAN SEA
WP
Western Region
NP
Northern Region
EP
Eastern Region

APPENDIX 4

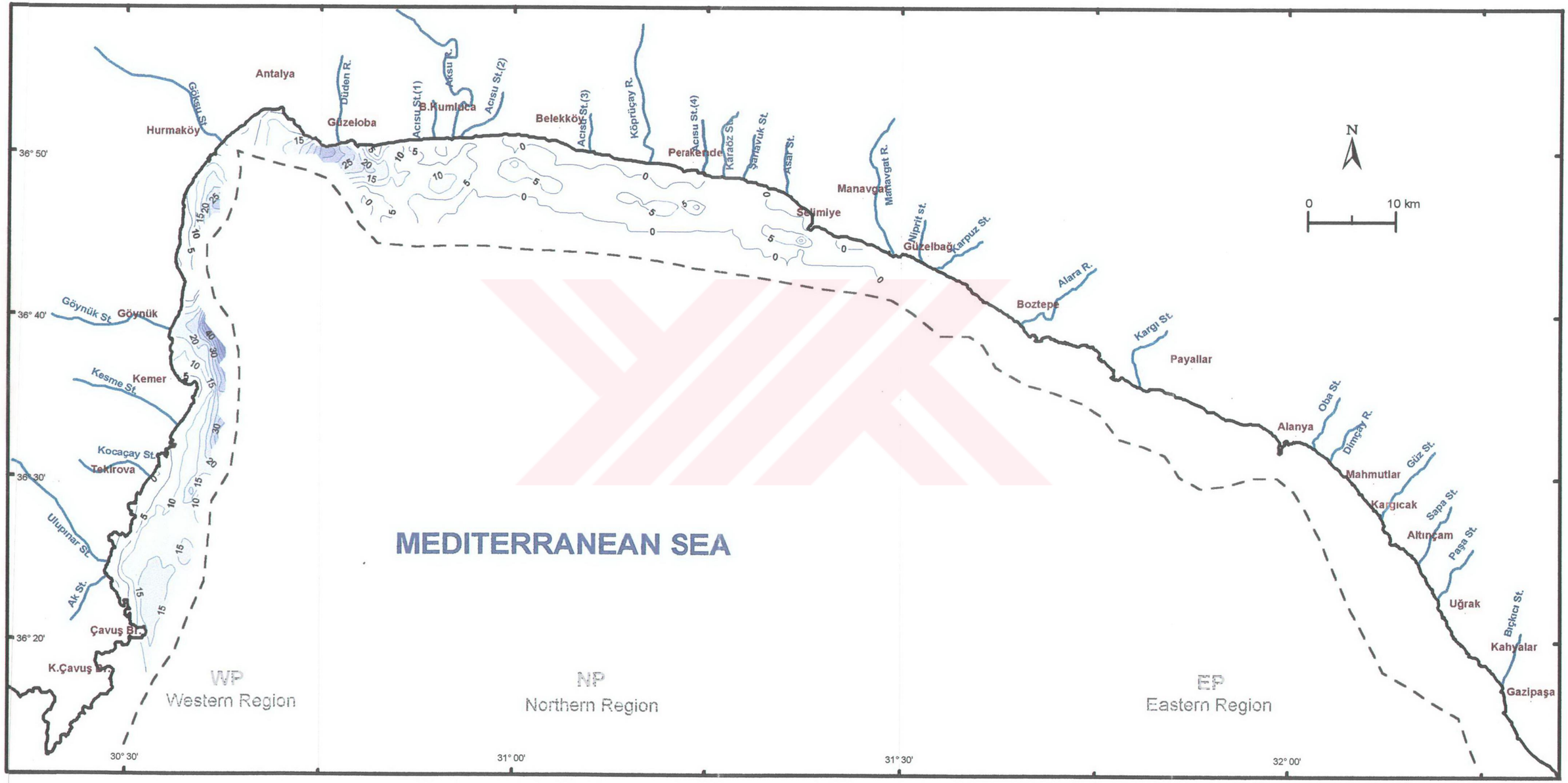
Antalya
Göksu St.
Hurmaköy
Düden R.
Güzeloba
Acısu St.(1)
B.Kumluca
Aksu R.
Acısu St.(2)
Belekköy
Acısu St.(3)
Köprüçay R.
Perakende
Acısu St.(4)
Karaöz St.
Yanavuk St.
Atsar St.
Manavgat
Manavgat R.
Selimiye
Nişprit st.
Karpuz St.
Güzelbağ
Alara R.
Boztepe
Kargı St.
Payallar
Oba St.
Alanya
Dimçay R.
Güz St.
Mahmutlar
Sapa St.
Kargıcak
Paşa St.
Altınçam
Uğrak
Bıçkıcı St.
Kahyalar
Gazipaşa
Göynük St.
Göynük
Kesme St.
Kemer
Kocaçay St.
Tekirova
Ulupınar St.
Ak St.
Çavuş Bl.
K.Çavuş Bl.
36° 50'
36° 40'
36° 30'
36° 20'
30° 30'
31° 00'
31° 30'
32° 00'
N
0
10 km
MEDITERRANEAN SEA
WP
Western Region
NP
Northern Region
EP
Eastern Region

APPENDIX 3

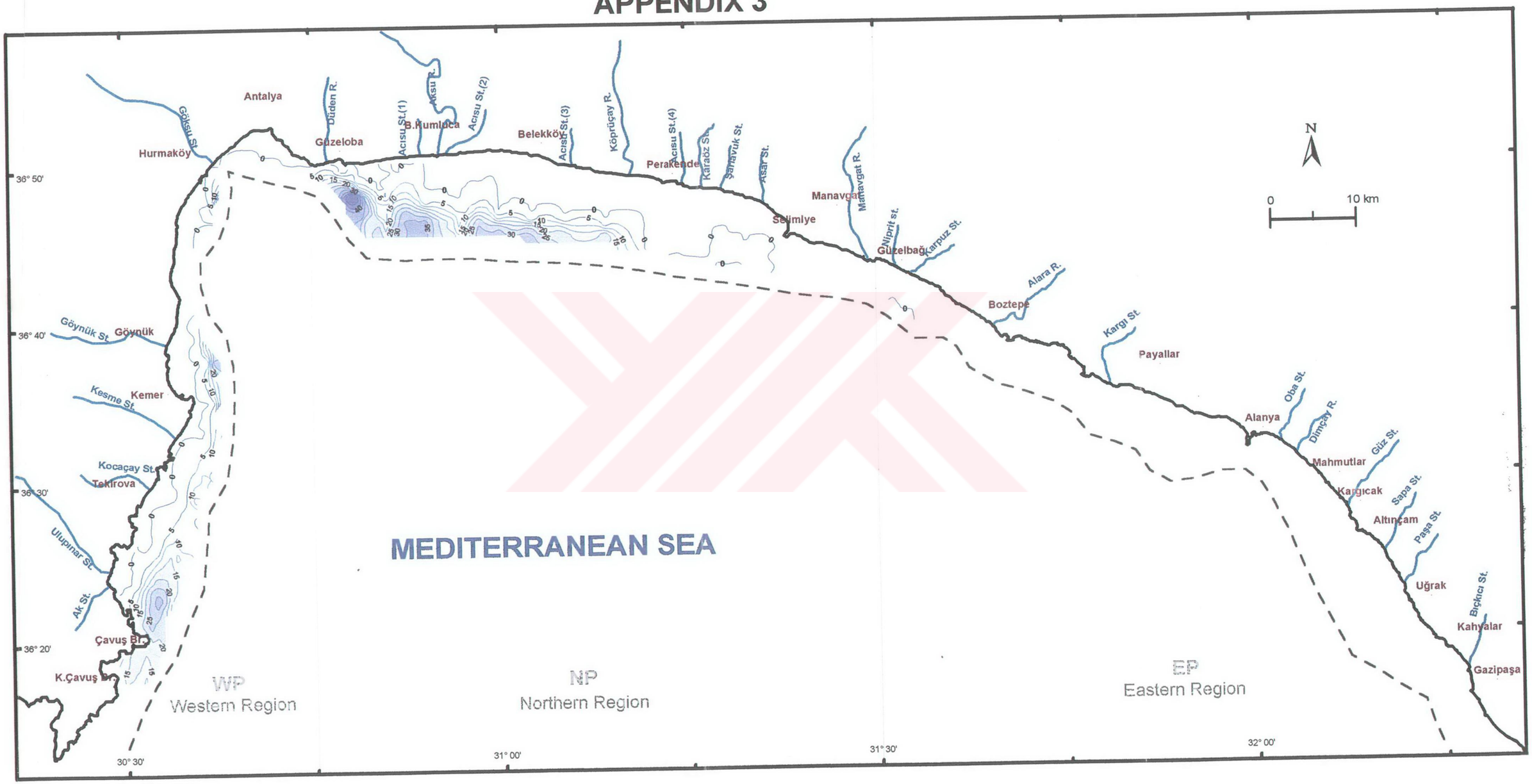
Antalya
Göksu St.
Düden R.
Acısu St.(1)
Aksu R.
Acısu St.(2)
B.Kumluca
Belekköy
Acısu St.(3)
Köprüçay R.
Acısu St.(4)
Karaöz St.
Sanavuk St.
Asar St.
Perakende
Manavgat
Manavgat R.
Selimiye
Nipnit st.
Güzelbağ
Karpuz St.
Alara R.
Boztepe
Kargı St.
Payallar
Oba St.
Alanya
Dimçay R.
Güz St.
Mahmutlar
Kargıcak
Sapa St.
Altınçam
Paşa St.
Uğrak
Birçınar St.
Kahyalar
Gazipaşa
Hurmaköy
Güzeloba
Göynük St.
Göynük
Kesme St.
Kemer
Kocaçay St.
Tekirova
Ulupınar St.
Ak St.
Çavuş Br.
K.Çavuş Br.
36° 50'
36° 40'
36° 30'
36° 20'
30° 30'
31° 00'
31° 30'
32° 00'
N
0
10 km
MEDITERRANEAN SEA
WP
Western Region
NP
Northern Region
EP
Eastern Region

APPENDIX 2

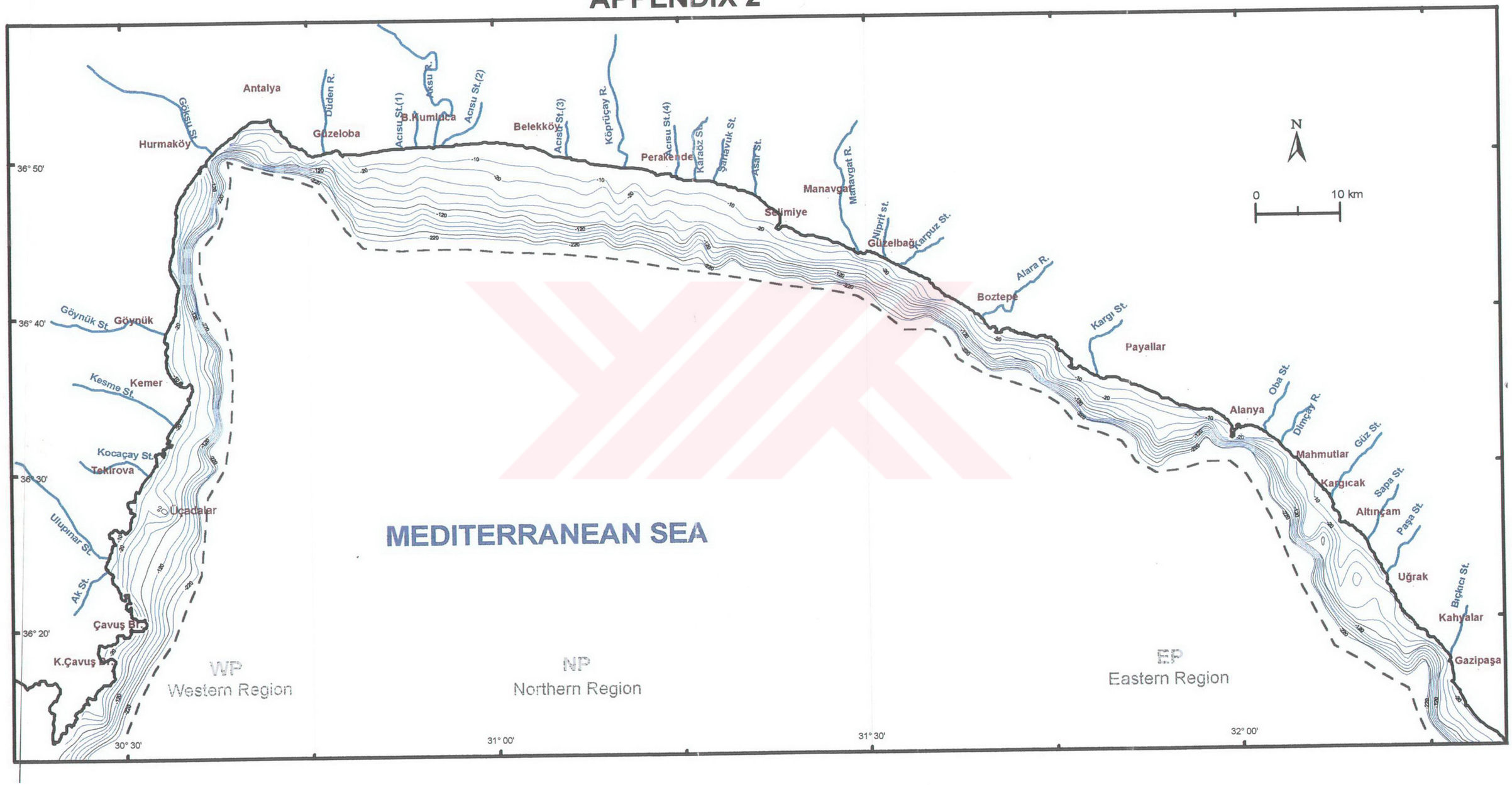
Antalya
Hurmaköy
Göksu St.
Düden R.
Güzeloba
Acısu St.(1)
B.Kumluca
Aksu R.
Acısu St.(2)
Belekköy
Acısu St.(3)
Köprüçay R.
Perakende
Acısu St.(4)
Karaöz St.
Yanavuk St.
Asar St.
Manavgat
Manavgat R.
Selimiye
Güzelbağ
Niprit st.
Karpuz St.
Alara R.
Boztepe
Kargı St.
Payallar
Oba St.
Alanya
Dimçay R.
Güz St.
Mahmutlar
Kargıcak
Sapa St.
Altınçam
Paşa St.
Uğrak
Bıçkıcı St.
Kahyalar
Gazipaşa
Göynük St.
Göynük
Kemer
Kesme St.
Kocaçay St.
Tekirova
Üçadalar
Ulupınar St.
Ak St.
Çavuş Bl.
K.Çavuş
36° 50'
36° 40'
36° 30'
36° 20'
30° 30'
31° 00'
31° 30'
32° 00'
N
0
10 km
MEDITERRANEAN SEA
WP
Western Region
NP
Northern Region
EP
Eastern Region

APPENDIX 1

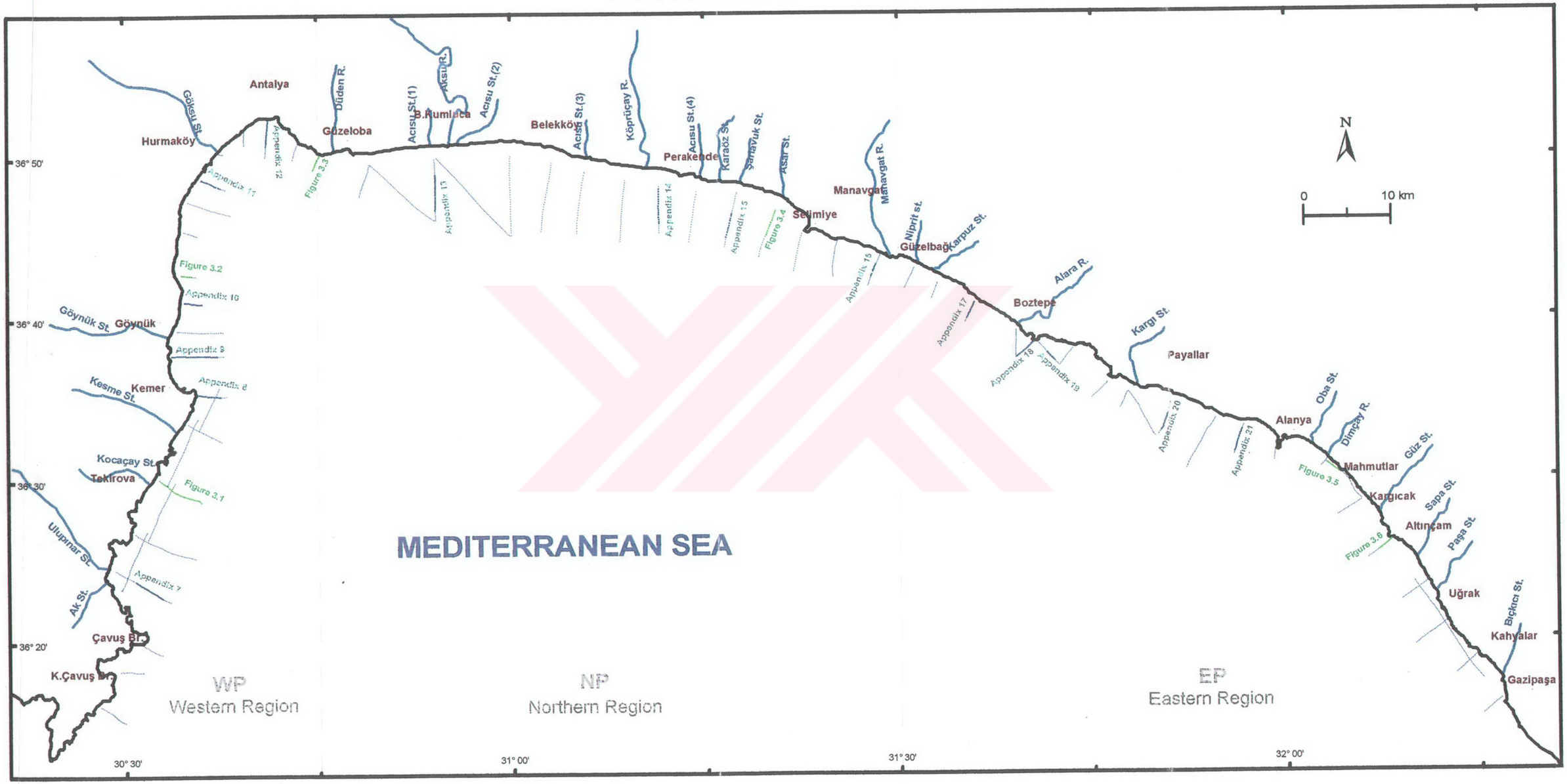

APPENDIX 8: High-resolution seismic profile (for location see Appendix 1) from the western region showing depositional sequences (1, 2, 3 and 4) and acoustic basement (AB). Note the reflector-R marks the pre-Holocene erosional surface. a : fan-delta progradation in depositional sequence 4.

APPENDIX 9: High-resolution seismic profile (for location see Appendix 1) from the western region showing depositional sequences (1, 2, 3 and 4) and acoustic basement (AB). Note the reflector-R marks the pre-Holocene erosional surface. a : fill seismic facies unit in depositional sequence 3.

APPENDIX 10: High-resolution seismic profile (for location see Appendix 1) from the western region showing depositional sequences (3 and 4) and acoustic basement (AB). Note the reflector-R marks the pre-Holocene erosional surface. a : fan-delta progradation in depositional sequence 4, b : fill seismic facies unit in depositional sequence 3.

APPENDIX 11: High-resolution seismic profile (for location see Appendix 1) from the western region showing depositional sequences (1, 2, 3 and 4) and acoustic basement (AB). Note the reflector-R marks the pre-Holocene erosional surface. a : fill seismic facies unit in depositional sequence 3.

APPENDIX 12: High-resolution seismic profile (for location see Appendix 1) from the western region showing depositional sequences (1, 3 and 4) and acoustic basement (AB). Note the reflector-R marks the pre-Holocene erosional surface, f-f': faults.

APPENDIX 18: High-resolution seismic profile (for location see Appendix 1) from the eastern region showing depositional sequence 4 and acoustic basement (AB). Note the reflector-R marks the pre-Holocene erosional surface. AW: acoustic window, f-f': faults.

APPENDIX 19: High-resolution seismic profile (for location see Appendix 1) from the eastern region showing depositional sequence 4 and acoustic basement (AB). Note the reflector-R marks the pre-Holocene erosional surface. f-f': fault.

APPENDIX 20: High-resolution seismic profile (for location see Appendix 1) from the eastern region showing depositional sequence 4 and acoustic basement (AB). Note the reflector-R marks the pre-Holocene erosional surface. Note also acoustic basement crops out at the sea floor, f-f': fault.

APPENDIX 21: High-resolution seismic profile (for location see Appendix 1) from the eastern region showing depositional sequence 4 and acoustic basement (AB). Note the reflector-R marks the pre-Holocene erosional surface. f-f': faults.

APPENDIX 13: High-resolution seismic profile (for location see Appendix 1) from the northern region showing depositional sequences (1, 2, 3 and 4) and acoustic basement (AB). Note the reflector-R marks the pre-Holocene erosional surface. Note also topset (TS) and forset beds (FS) in depositional sequence 2.

APPENDIX 14: High-resolution seismic profile (for location see Appendix 1) from the northern region showing depositional sequences (1, 3 and 4) and acoustic basement (AB). Note the reflector-R marks the pre-Holocene erosional surface. a: fill seismic facies unit in depositional sequence 4.

APPENDIX 15: High-resolution seismic profile (for location see Appendix 1) from the northern region showing depositional sequence 4 and acoustic basement (AB). Note the reflector-R marks the pre-Holocene erosional surface, f-f': faults.

APPENDIX 16: High-resolution seismic profile (for location see Appendix 1) from the northern region showing depositional sequence 4 and acoustic basement (AB). Note the reflector-R marks the pre-Holocene erosional surface. a: fill seismic facies unit in depositional sequence 4, f-f': faults.

APPENDIX 17: High-resolution seismic profile (for location see Appendix 1) from the eastern region showing depositional sequence 4 and acoustic basement (AB). Note the reflector-R marks the pre-Holocene erosional surface. a: fill seismic facies unit in depositional sequence 4, f-f': fault.

APPENDIX 19

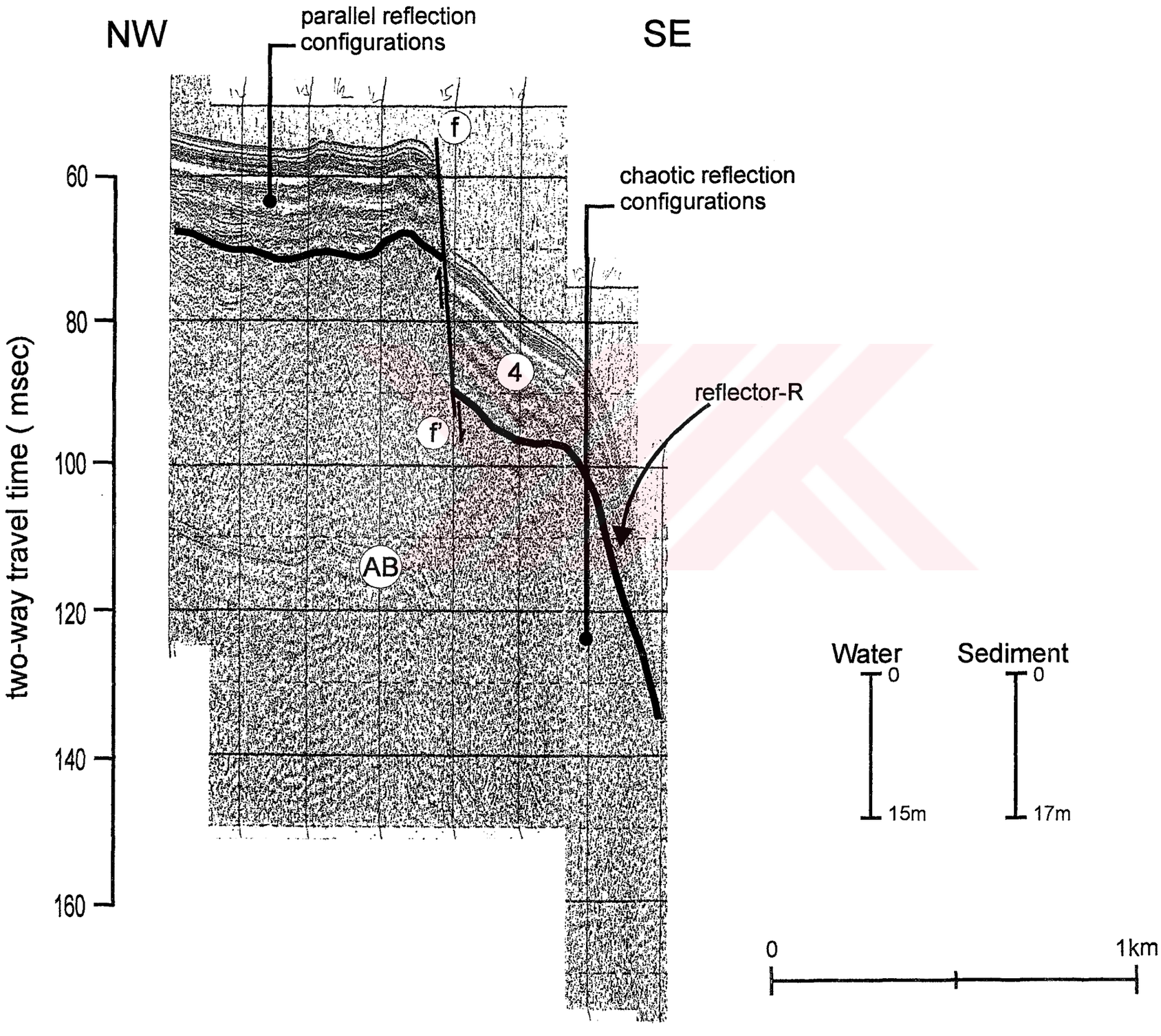
NW
parallel reflection configurations
SE
chaotic reflection configurations
reflector-R
f
f'
4
AB
two-way travel time (msec)
60
80
100
120
140
160
Water
0
15m
Sediment
0
17m
0
1km

APPENDIX20

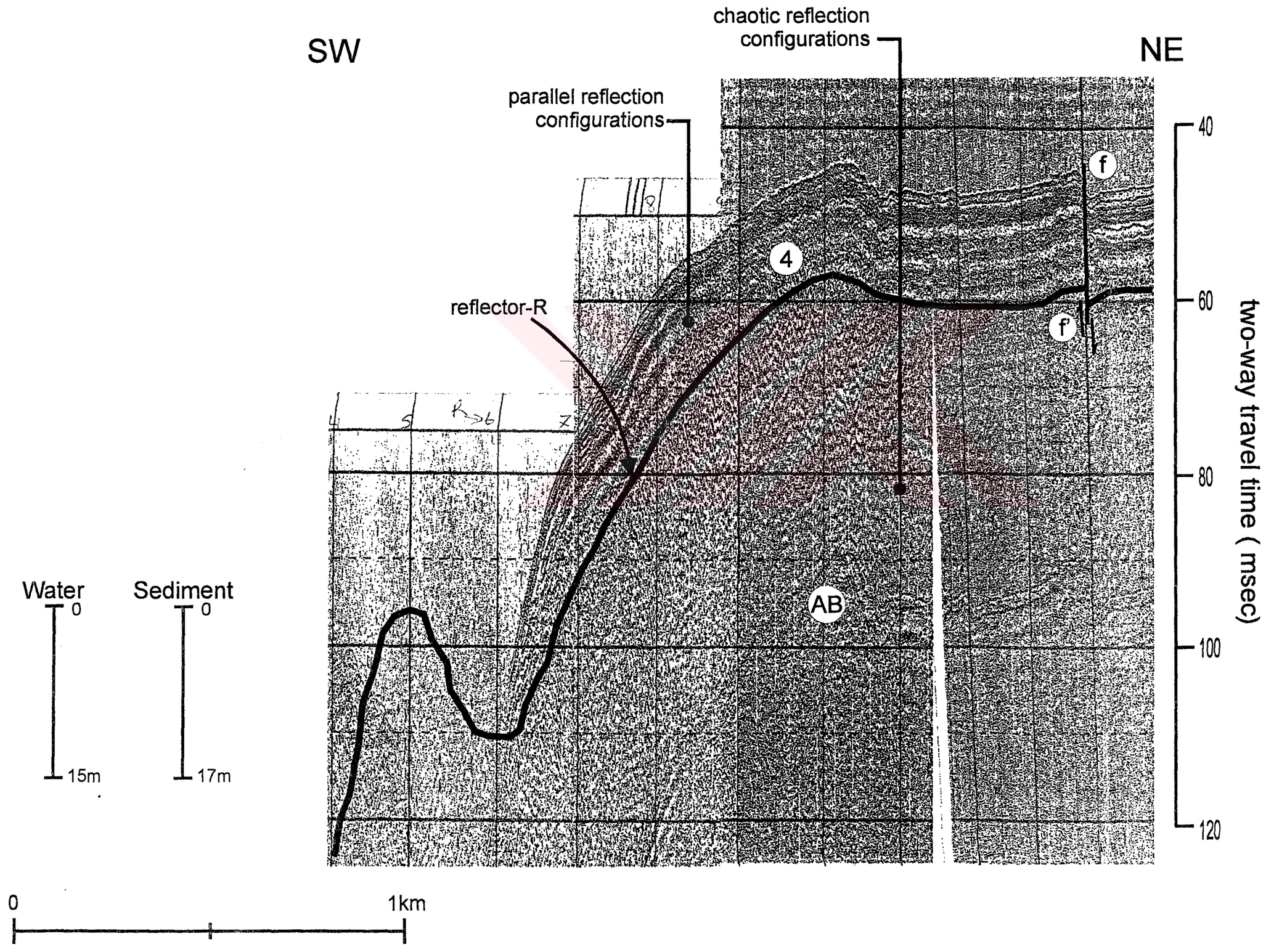
SW
NE
chaotic reflection configurations
parallel reflection configurations
reflector-R
4
f
f'
AB
40
60
80
100
120
two-way travel time (msec)
Water
0
15m
Sediment
0
17m
0
1km

APPENDIX 21

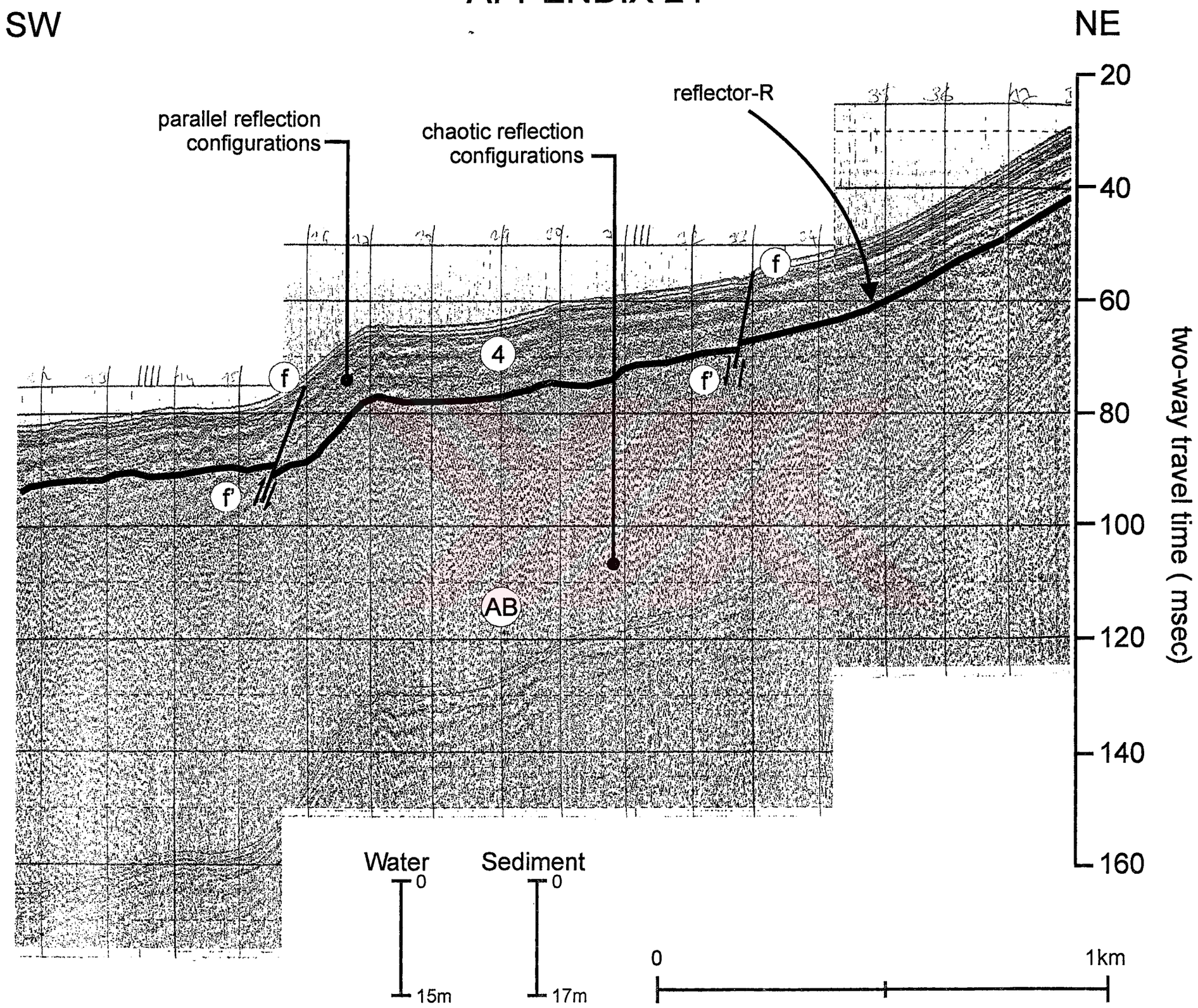
SW
NE
parallel reflection configurations
chaotic reflection configurations
reflector-R
f
f'
4
AB
20
40
60
80
100
120
140
160
two-way travel time (msec)
Water
0
15m
Sediment
0
17m
0
1km